Arabian Journal of Geosciences (2019) 12: 773
https://doi.org/10.1007/s12517-019-4872-4

ORIGINAL PAPER

Soft-sediment deformation: deep-water slope deposits of a back-arc basin (middle Eocene-Oligocene Kırkgeçit Formation, Elazığ Basin), Eastern Turkey

Calibe Koç-Taşgın[1] · Fırat Altun[2]

Received: 7 March 2019 / Accepted: 3 October 2019 / Published online: 10 December 2019

Abstract

The Kırkgeçit Formation (middle Eocene-Oligocene) is exposed in an approximately E-W direction around the city of Elazığ, eastern Turkey. This unit represents marly and sandy deep-marine sediments deposited in a slope setting with channels and contain soft-sediment deformation structures (SSDSs). These SSDSs include slump folds, chaotic strata, load casts, flame structures, convolute laminations, clastic dykes, water-escape structures and syn-sedimentary faults. The main underlying deformation processes are liquefaction, fluidization and gravity-induced loading. Some of the SSDS could be interpreted as seismites, which originated due to earthquakes that also triggered high-density mass flows. This interpretation is consistent with the active tectonics in the Elazig back-arc basin. The SSDS in the study area are compared with SSDS in other regions, as well as with SSDS in other marine deposits. In this way, findings obtained from the study area are compared with SSDS at different locations in the marine Kırkgeçit Formation around Elazığ and with similar structures developed in marine settings worldwide, such as SE Crete and NW Africa.

Keywords Soft-sediment deformation structures · Deep-water · Slope · Back-arc setting · Elazığ Basin · Turkey

Introduction

The shallow- and deep-marine facies of the Kırkgeçit Formation in the Eastern Anatolia region (around Malatya, Elazığ and Van) are observed near Elazığ (Figs. 1 and 2). Three stages have been developed in Elazığ Basin since the end of late Cretaceous due to plate movements. Firstly, the Elazığ Basin developed at the end of the Late Cretaceous and was affected by the compressive tectonic regime in the region (Fig. 2). Permo-Triassic Keban metamorphic rocks and Upper Cretaceous Elazığ magmatic rocks form the basement of the basin. From the end of the Late Cretaceous to the Palaeocene, the Upper Taurus magmatic arc was overlain by older metamorphic rocks following the closure of the Inner Tauride Ocean (Bingöl 1984; Hempton 1985; Yazgan and Chessex 1991; Turan et al. 1995; Aksoy et al. 2005). Continental areas developed due to regional uplift (Pertek thrust fault). In this tectonically controlled basin, clastic alluvial fan and evaporitic playa sediments (Kuşçular Formation) were deposited. Secondly, marine sediments transgressively overlay the alluvial fan deposits in the late Palaeocene and early Eocene (Seske Formation) in the extensional regime. During this period, the sea advanced northward in the basin affected by block faulting in an extensional back-arc environment (Fig. 2). In the middle-late Eocene, the sea was at its maximum width (Kırkgeçit Formation in the Elazığ area). In the Oligocene-Miocene, the sea retracted towards the N-NW and the southern area gradually became shallower (Aksoy et al. 2005). It is accepted by various researchers that the Kırkgeçit Basin developed as a back-arc basin on the continental crust in the middle Eocene and that the base was controlled by block faulting (Turan et al. 1995). In the study area,

Responsible Editor: Beatriz Badenas

✉ Calibe Koç-Taşgın
calibekoc@firat.edu.tr

Fırat Altun
firat_altun85@hotmail.com

[1] Department of Geological Engineering, Fırat University, 23119 Elazığ, Turkey

[2] Institute of Science, Fırat University, 23119 Elazığ, Turkey

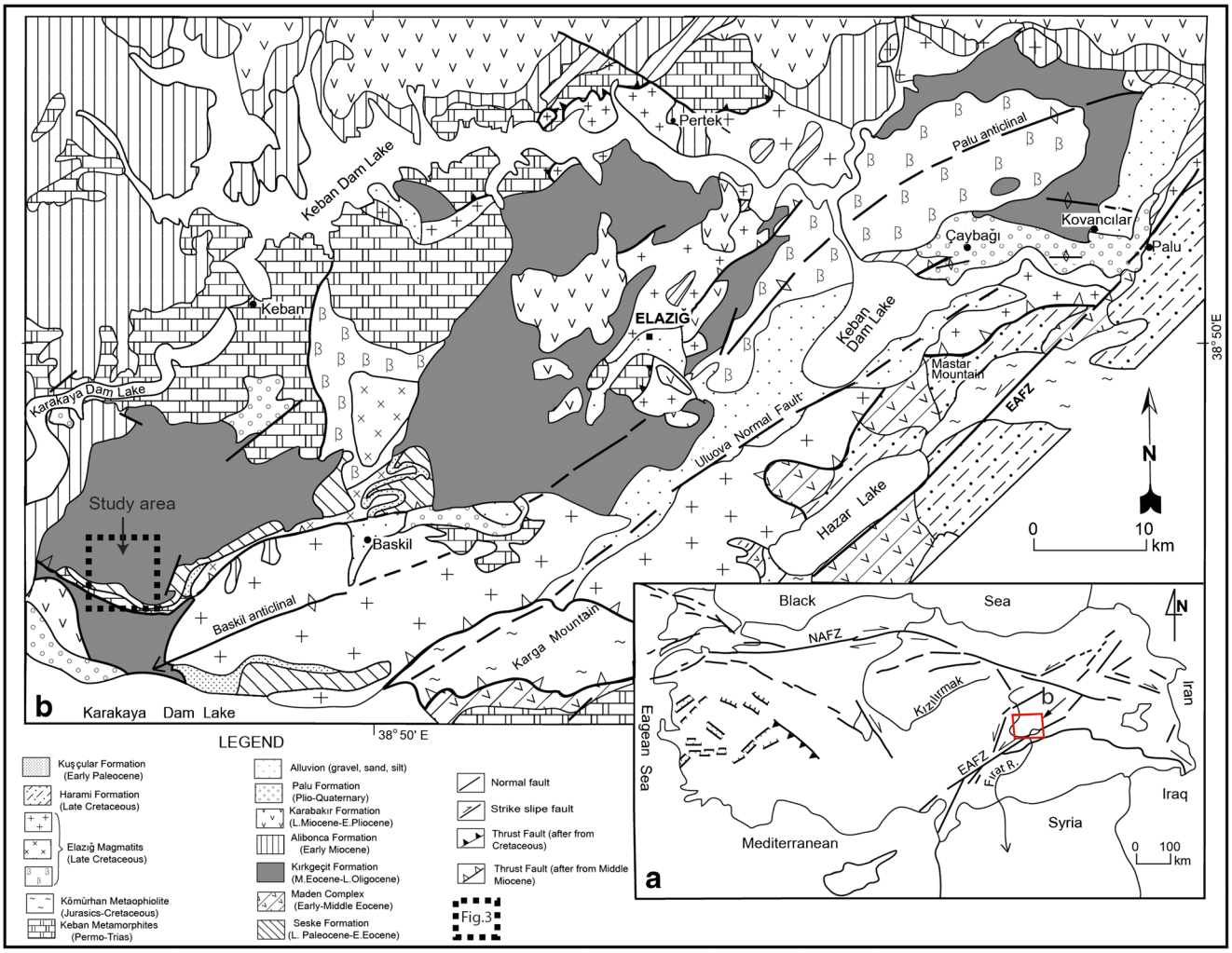

Fig. 1 **a** Simplified structural map of Turkey and location of the study area (red rectangle). **b** Geological map of the Elazığ Basin (East Anatolia) (modified from Turan 1993)

large-sized olistolith blocks derived from the marbles of the Keban metamorphic rocks have been identified at the lowermost part of the Kırkgeçit Formation, indicating also a strong tectonic control (Fig. 3). Thirdly, regional uplift following the closure of the Neo-Tethys and regional continent-continent collision in the middle Miocene indicate the beginning of

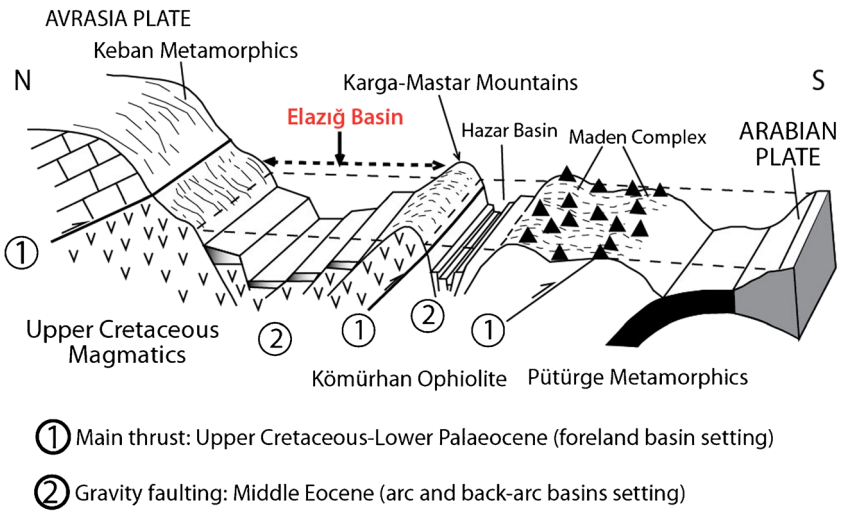

Fig. 2 Cartoon of the palaeogeography of the Elazığ Basin (Yazgan 1984; Özkul 1988; Aksoy et al. 2005)

the neotectonic stage (Şengör 1980; Şengör and Yılmaz 1983; Dewey et al. 1986; Hempton 1987). As a result of north-south directional compression, folds and thrust faults were formed in the Palaeogene units.

Soft-sediment deformation structures are records of sedimentary and tectonic processes in many sedimentary environments (Mazumder et al. 2016; Neuwerth et al. 2006; Spalluto et al. 2007; Basilone et al. 2014; Rossetti et al. 2017; Brogi

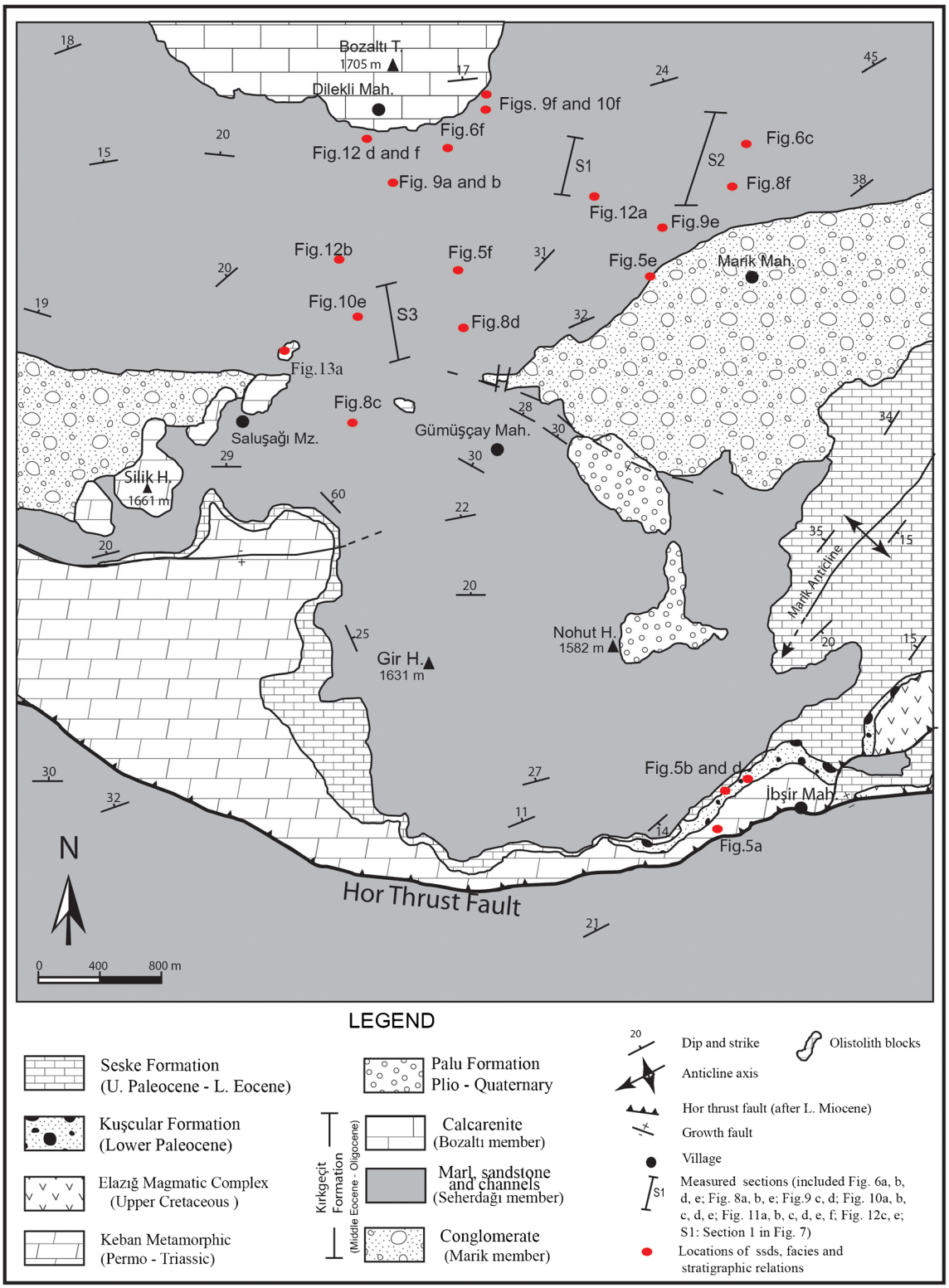

Fig. 3 Detailed geological map of the study area and points of stratigraphic measured sections and SSDS (modified from Turan 1984 and Cronin et al. 2005)

et al. 2018; Alves 2015). These structures form during/shortly after sedimentation and before the consolidation of sediments is complete. For example, they have been reported in continental environments (Hempton and Dewey 1983; Karlin and Abella 1992; Scott and Price 1988; Alfaro et al. 1997; Jones and Omoto 2000; Rodríguez-Pascua et al. 2000; Neuwerth et al. 2006; Koç-Taşgın and Türkmen 2009; Koç-Taşgın 2011; Koç-Taşgın et al. 2011; Koç-Taşgın and Diniz-Akarca 2018; Koç-Taşgın et al. 2018), transitional settings (Bhattacharya and Bandyopadhyay 1998; Gibert et al. 2005; Owen and Moretti 2008; Bhattacharya and Bhattacharya 2010) and marine successions (Johnson 1977; Molina et al. 1998; Rossetti 1999; Rossetti et al. 2000; Rossetti and Goes 2000; Moretti et al. 2001; Greb and Archer 2007; Alves and Lourenço 2010; Kangi et al. 2010; Mastrogiacomo et al. 2012; Chen and Lee 2013; Yamamoto 2014; Alves 2015; Ortner and Kilian 2016; Altun 2018).

The soft-sediment deformation structures in the Kırkgeçit Formation in Elazig basin studied in the present work (Figs. 2 and 3) were developed in deep-marine sediments. Various deformation structures and facies occurring due to different triggering mechanisms have been defined in deep-sea sediments (Alves et al. 2007; Alves and Lourenço 2010; Yamamoto 2014; Basilone et al. 2014; Alves 2015; Gamboa and Alves 2015; Ge and Zhong 2017; Alves and Cupkoviç 2018; Gladstone et al. 2018). Oliveira et al. (2009) and Yamamoto (2014) recognized aseismically induced asymmetrical soft-sediment deformation structures of submarine slope and trench slope deposits caused by liquefaction triggered by slope instability. Alves et al. (2007) and Alves and Lourenço (2010) emphasized the deformation styles of late Miocene submarine failures in SE Crete, eastern Mediterranean. Basilone et al. (2014) associated the formation of soft-sediment deformation occurring in deep-water carbonate successions with repeated events related to the late rifting processes of the African continental margin. Alves (2015) reviewed the significance of submarine slide blocks and associated soft-sediment deformation structures in deep-water stratigraphic successions (to Cenozoic from Precambrian) throughout the world, from eastern Canada to the South Atlantic, Australia and the Gulf of Mexico. Ge and Zhong (2017) defined soft-sediment deformation structures in early Cretaceous aged outer fan deposits consisting of debrite, turbidite and deformed sediments, linked to seismic activity associated with active tectonism and volcanism and Early Cretaceous anoxic events. Alves and Cupkoviç (2018) stated that the mass transport of sediments was ubiquitous on tectonically active slopes with coarse-grained sediments to heterolithic mass-transport deposits and silty-sandy turbidites.

Soft-sediment deformation structures in the middle Eocene-Oligocene marine sediments (Kırkgeçit Formation) have not been studied in detail until now in the Elazığ area studied here (eastern Turkey; Fig. 2). Koç-Taşgın and Altun (2019) described slump sheets extending for 5 km within near-shelf calcarenite-carbonate mudstone alternations in the same unit north of this study area (6 km outside of the map area in Fig. 3). They concluded that these structures are seismically induced slumps according to some criteria, such as lateral continuity and tectonic setting.

The sedimentological study of Kırkgeçit Formation presented here aims to (i) identify the type of soft-sediment deformation structures and their deformation mechanisms, (ii) document the depositional conditions of the deep-water slope deposits, (iii) discuss different triggering mechanisms that may form these structures, and (iv) demonstrate the active tectonic control of sedimentation in the Elazığ Basin and its seismicity. Consequently, all these findings are compared with similar structures in different deep-water slope deposits obtained from previous studies (e.g. Alves et al. 2007; Oliveira et al. 2009; Alves and Lourenço 2010; Basilone et al. 2014; Yamamoto 2014; Alves 2015; Gamboa and Alves 2015; Ge and Zhong 2017; Alves and Cupkoviç 2018; Gladstone et al. 2018).

Geological setting

The Elazığ Basin is one of the basins developed during the closing of the southern branch of the Neo-Tethys in the Paleogene. The basin, stretching in the NE-SW direction, is located in the Eastern Taurus (Figs. 1 and 2). The Kırkgeçit Formation represents a transgressive unit covering older rocks and crops out from 25 km west of Elazig (Baskil) to 60 km east (Kovancılar) in a wide area (Fig. 1).

The stratigraphic, sedimentological and tectonic features of the unit are discussed in several previous studies (Perinçek 1979; Bingöl 1984; Turan 1984; Özkul 1988; Turan et al. 1995; Özkul and Kerey 1996; Türkmen et al. 2001; Turkmen and Erturk 2002; Cronin et al. 2005). The deep-water and shelf sediments of the Kırkgeçit Formation were deposited during rapid basin subsidence in the back-arc environment blocked by normal faults. The formation is characterized by shelf facies (calcarenite) in the north (Türkmen and Esen 1997) and slope and basin plain facies in the south in the Elazığ region (Özkul and Kerey 1996).

The Keban metamorphic rocks (Permo-Triassic) and Elazığ magmatic rocks (Late Cretaceous) constitute the basement of the study area (Figs. 3, 4 and 5a). They are overlain by the early Palaeocene terrestrial Kuşcular Formation, late Palaeocene-early Eocene marine Seske Formation, middle Eocene-Oligocene Kırkgeçit Formation and Plio-Quaternary Palu Formation (Figs. 3 and 4). The Kuşcular Formation is a unit consisting of alluvial fan deposits in front of a major thrust fault (Pertek thrust fault) (Fig. 5b). The intraformational unconformity developed in the distal part of alluvial fan deposits, and the soft-sediment deformation structures were

formed due to the tectonic deformation and seismic activity occurring here (Koç-Taşgın 2017) (Fig. 5c). The Seske Formation, which is the first product of the Paleogene transgression, unconformably overlies the early Palaeocene conglomerates (Fig. 5d). The unit, which starts with sandy limestones at the bottom, passes into limestones towards the top, and the thickness varies from place to place. This stratigraphic position indicates that the extent of the Neo-Tethys was controlled by the tectonic and topographic features of the region in the Eocene. In addition, some parts of this region were

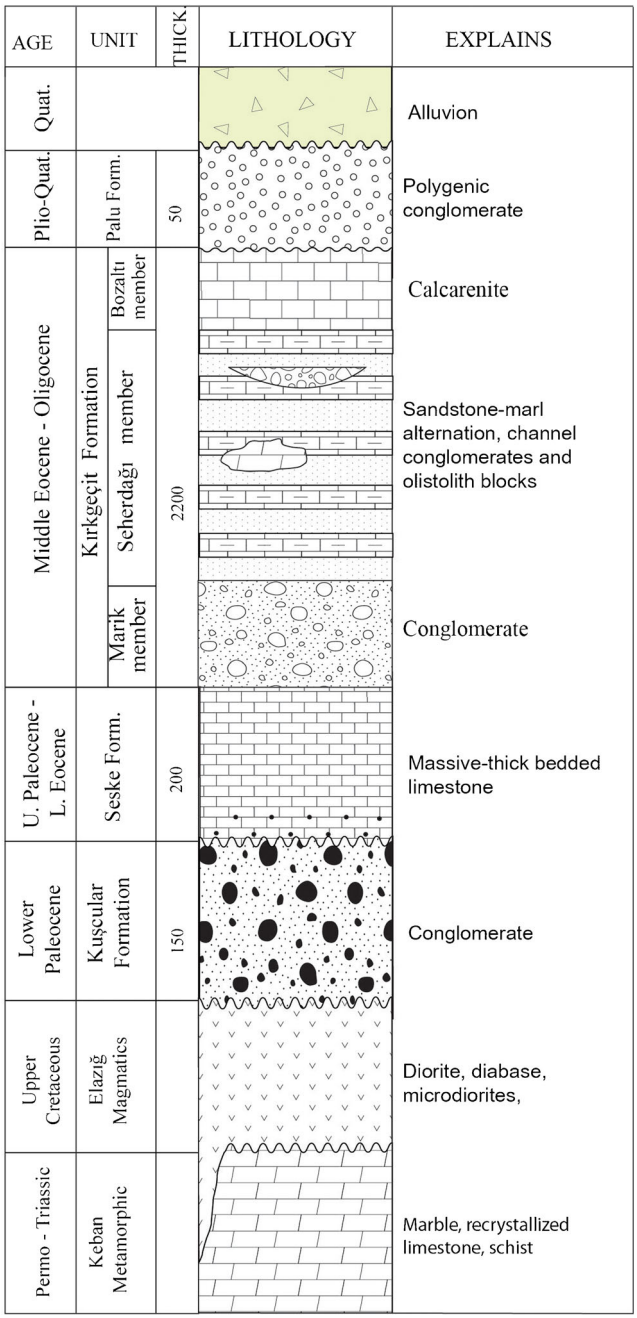

Fig. 4 Generalized stratigraphic section of the study area (modified from Turan 1984)

under subaerial conditions in the late Palaeocene and early Eocene (Türkmen et al. 2001). The Palu Formation (Plio-Quaternary) is the youngest unit of the study area and consists of immature and grain-supported conglomerate with a mud matrix.

The Kırkgeçit Formation overlies conformably the Seske Formation and is divided into three members in the study area (Marik, Seherdağı and Bozaltı members from base to top; Figs. 3 and 4). The Marik member is not observed along the whole base of the unit and is composed of conglomerates with variegated colours and medium-thick stratification (Fig. 5e). The main sources of the gravels of these conglomerates are the Keban metamorphic rocks and Elazığ magmatites, and there are also some limestone pebbles belonging to the Harami Formation. As a result of the investigations carried out in this unit, no soft-sediment deformation structures were observed. The Seherdağı member (Fig. 5f) reflects slope environments dominated by mud and includes complex channel facies that become shallower to the north. The soft-sediment deformation structures described in this study are specific to this member. The slope deposits are covered by the Bozaltı member consisting of the prograding shelf sands (calcarenites) (Figs. 3 and 4). These sands are correlated with middle Eocene (Bartonian) thick-bedded massive limestones north of the study area (Türkmen and Ertürk 2002; Koç-Taşgın and Altun 2019). Sedimentological and petrographic studies conducted in thick limestones have revealed that the unit was deposited on a carbonate shelf.

Properties of facies containing soft-sediment deformation structures

Six facies belonging to the Seherdağı Member of the Kırkgeçit Formation have been defined in the study area (Figs. 6 and 7). Its vertical distribution in three selected sections is included in Fig. 7

Facies 1: sand matrix-supported conglomerates

Description: The facies is represented by massive, sand matrix-supported conglomerates with lenticular geometry and erosional bases (Fig. 6a, b). This facies passes to massive sandstone facies and stratified sandstone facies both laterally and vertically (Fig. 6b). These changes usually show sharp contacts. The maximum thickness measured in the sections is 13 m (section 3 in Fig. 7). The maximum grain size is 30 cm, with an average of 7–8 cm. The gravels are mostly well rounded with very few corners and consist of mainly magmatic and smaller amounts of metamorphic rock fragments. The matrix is composed of sand and fine gravel. Palaeo-flow directions taken from the clast imbrication observed in the conglomerates are towards 200–223°.

Interpretation: The conglomerates with erosional-based, matrix-supported lenticular geometry represent deeply cut channels (Ge and Zhong 2017; Alves and Cupkoviç 2018). In high-density turbulent flows, the conglomerates are interpreted as laminar cohesive debris flows or deposits from suspension (Lowe 1982).

Facies 2: mud matrix-supported conglomerates

Description: The thickness of this facies, which related laterally and vertically with marl facies, is approximately 2 m (Fig. 6c). The pebbles are dispersed in the marl, and the maximum gravel length is up to 10 cm. At some levels, the mud proportion is considerably higher than the gravel rate. Slump folds have been observed also in this facies.

Interpretation: Some pebbly muds may occur as a result of the gravel and slurry falling down the steep slopes into the mud (Lowe 1982; Marjanac 1985; Alves and Lourenço 2010; Alves 2015). Debris sediments could be rich in mud and sand or be a mixture of both. Debris flows have the ability to transport gravel and coarse sands (due to their strength), and such deposits are defined as debrite (Shanmugam 2016). The gravelly marl deposits described here are debrites.

Facies 3: massive sandstones

Description: Massive sandstones with an average thickness of 1.5–2 m are generally associated with matrix-supported conglomerates. They extend laterally and contain gravel levels. No structures are observed in this facies.

Interpretation: Sand flow or other grain flow processes on steep slopes may settle massive sands. Such units can occur as a result of rapid sedimentation from high-concentration turbidite currents (Middleton 1969; Aalto 1976; Lowe 1976; Hiscott and Middleton 1979; Lowe 1982).

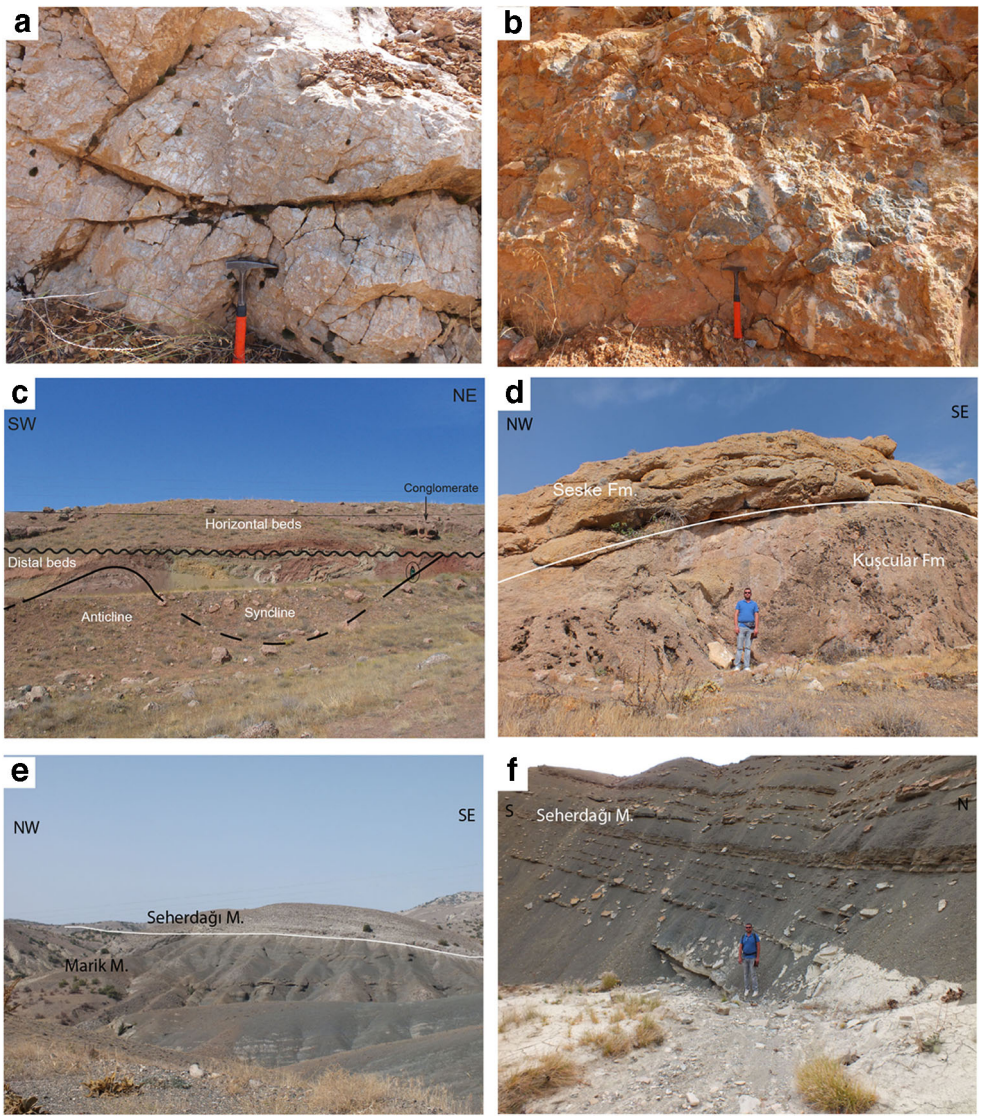

Fig. 5 Outcrop photographs of lithostratigraphic units from the study area in the Elazığ Basin. **a** Keban metamorphic rocks composed of marble. **b** Kuşçular Formation, red-coloured conglomerate on a proximal fan. **c** Distal fan deposits of the Kuşçular Formation containing soft-sediment deformation structures related to a syn-tectonic intraformational unconformity (Koç-Taşgın 2017). **d** Seske Formation represented by limestone overlying the Kuşçular Formation. **e** Marik member. **f** Seherdağı member showing marl intercalated with sandstone

Facies 4: stratified sandstones

Description: Theses sandstones are thin- to medium-bedded (10–40-cm-thick beds) and have fine to medium grain size. They usually have lateral continuity, but some stratified sandstones observed on top of the conglomerate channel facies have lenticular geometry (Fig. 6a, b). This facies has no sedimentary structures and is observed alternating with marls in places.

Interpretation: This facies probably formed by the precipitation of finer drift springs developing successively in the base of high-density turbidite currents (Mutti and Ricci Lucchi 1975; Pickering et al. 1986).

Facies 5: normally graded sandstones

Description: This facies is formed by fine- to medium-grained and thin-bedded sandstones (bed thickness of 15–35 cm) and is only locally present (Fig. 6d). Parallel lamination and normal grading can be recognized at some levels and base structures (flute marks and load casts) are rarely present (Fig. 6e).

Interpretation: This facies occurs as a result of rapid deposition and rapid burial of particles in suspension in high-density turbidite flows (Hubert et al. 1970; Stanley et al. 1978; Watson 1981; Hein 1982) and can form part A of the Bouma sequence.

Facies 6: marls

Description: The thickness of the marl facies varies between 10 and 50 m. This facies includes fine-grain, thin-bedded sandstone (Facies 4) intercalations (sandstone/marl ratio is 1/10). The marls have parallel lamination and contain planktonic foraminifera (*Globigerina* sp. and *Globorotalia* sp.).

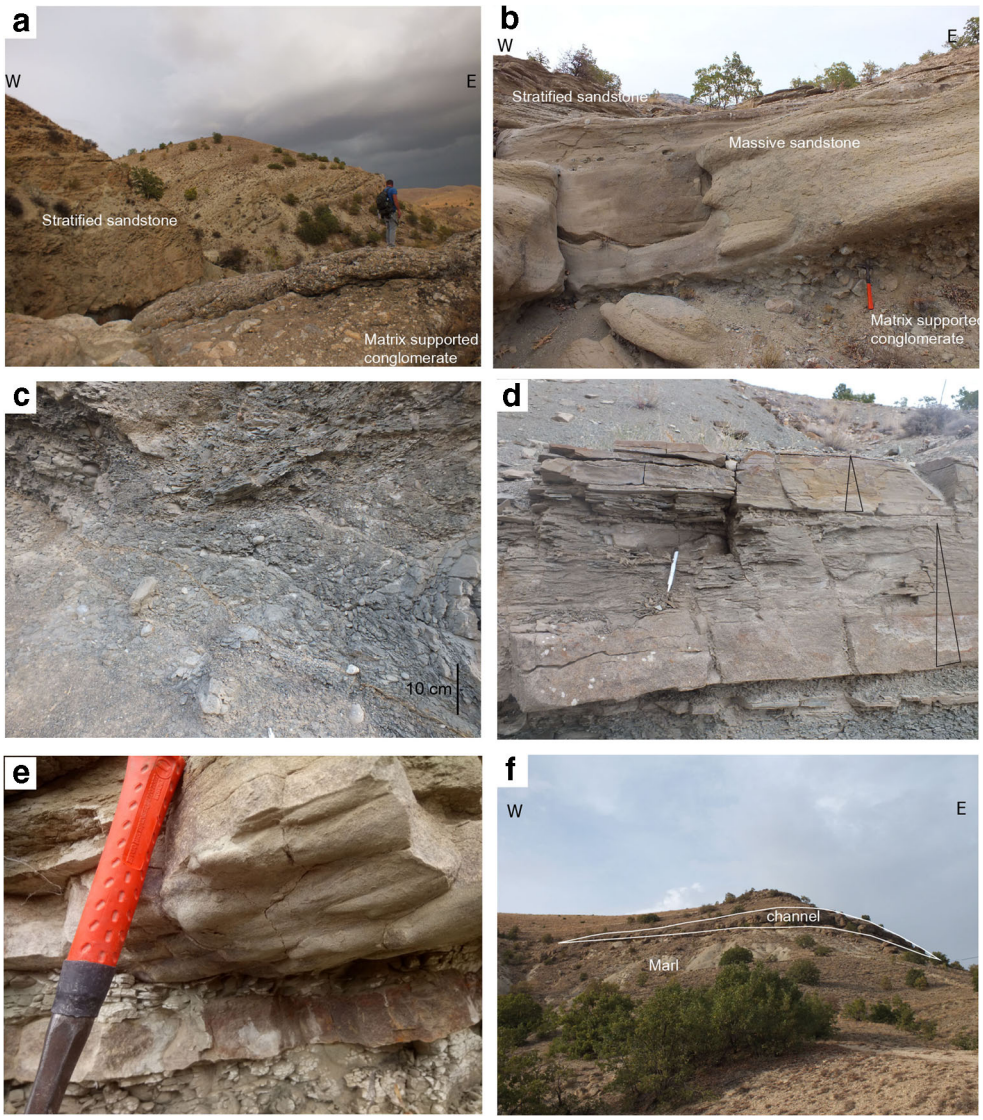

Fig. 6 Outcrop photographs of the sedimentary facies of the Kırkgeçit Formation in the study area. **a** Sand matrix-supported conglomerate and stratified sandstones (channel deposits). **b** Massive conglomerate, massive sandstone and stratified sandstones (lenticular geometry channel deposits). **c** Mud matrix-supported conglomerates. **d** Flute marks observed at the base of sandstone. **e** Normally graded sandstone. **f** Channel deposits that show lenticular geometry

Interpretation: Laminated mudstones represent pelagic-hemipelagic deposition from suspension settling in an open-marine setting, from high turbidity currents and/or by deep ocean currents or shear processes. This precipitation may be associated with relatively rapid deposition (Cremer and Stow 1986; Stow et al. 1986).

Soft-sediment deformation structures

Multiple soft-sediment deformation structures are observed in the Seherdağı Member of the Kırkgeçit Formation. These structures are slump folds, chaotic strata, load casts, flame structures, convolute laminations, clastic dykes, water-escape structures and syn-sedimentary faults.

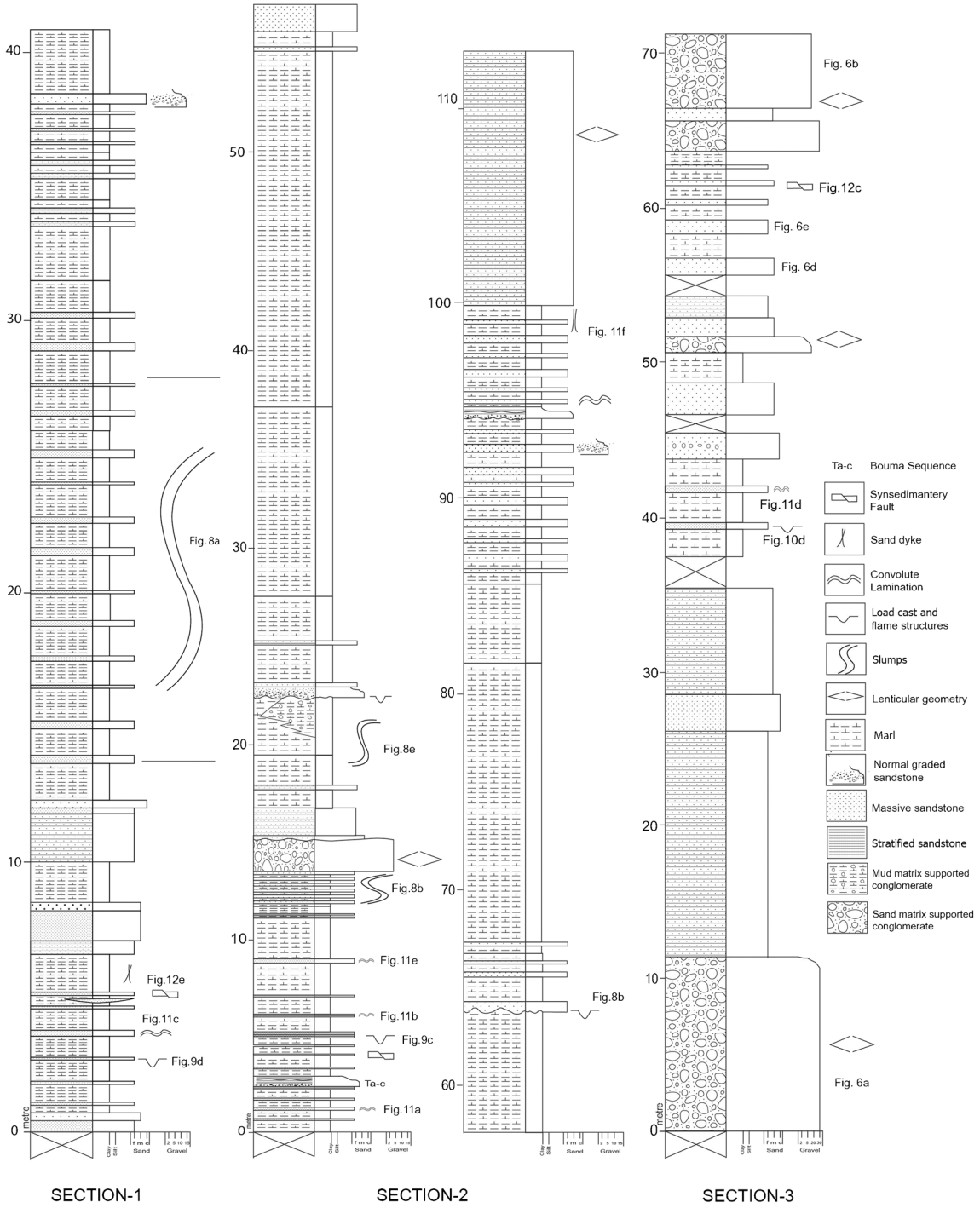

Fig. 7 Stratigraphic sections measured in the Kırkgeçit Formation, showing sedimentary facies and the occurrence of some soft-sediment deformation structures

Slump folds

Description: Slumps with different morphologies are commonly observed in sandstone-marl alternations, mud matrix-supported conglomerates and marls (Figs. 7 and 8). These structures are generally at metre scale (2–15 m). Occasionally, they are horizontal and sometimes irregular folds. Deformed beds with slumps are overlain and underlain by undeformed beds. The movement direction from the slump sheets varies between 200° and 250°. The dip of the axial plane of the folds normally shows the direction of the 'source' of the slump sheet. Small-scale faults are observed in the core part of the slumps.

Interpretation: These structures are associated with the downslope movement of unlithified sediments under the influence of gravity. When the stratified sediments steepen, they slip due to the increase past the angle of stability (Mills 1983; Alves and Lourenço 2010; Alsop and Marco 2011; Alves 2015). In the delta environments, the presence of low-permeability silt and clays supporting high porewater pressure facilitates the formation of slump movement (Morgenstern 1967). In the deep-marine sediments studied here, this effect was probably due to the marl facies that are intercalated with the sandstones.

Chaotic strata

Description: Chaotic strata have a thickness of approximately 20, are composed of densely folded, disturbed, fragmented layers and exhibit rather mixed morphologies (Fig. 9a, b). In curved structures, fold axial planes are observed in horizontal, vertical and oblique positions and are confined to deformed layers.

Interpretation: Fractured and disturbed beds characterize less consolidated and less water-saturated sediments, while

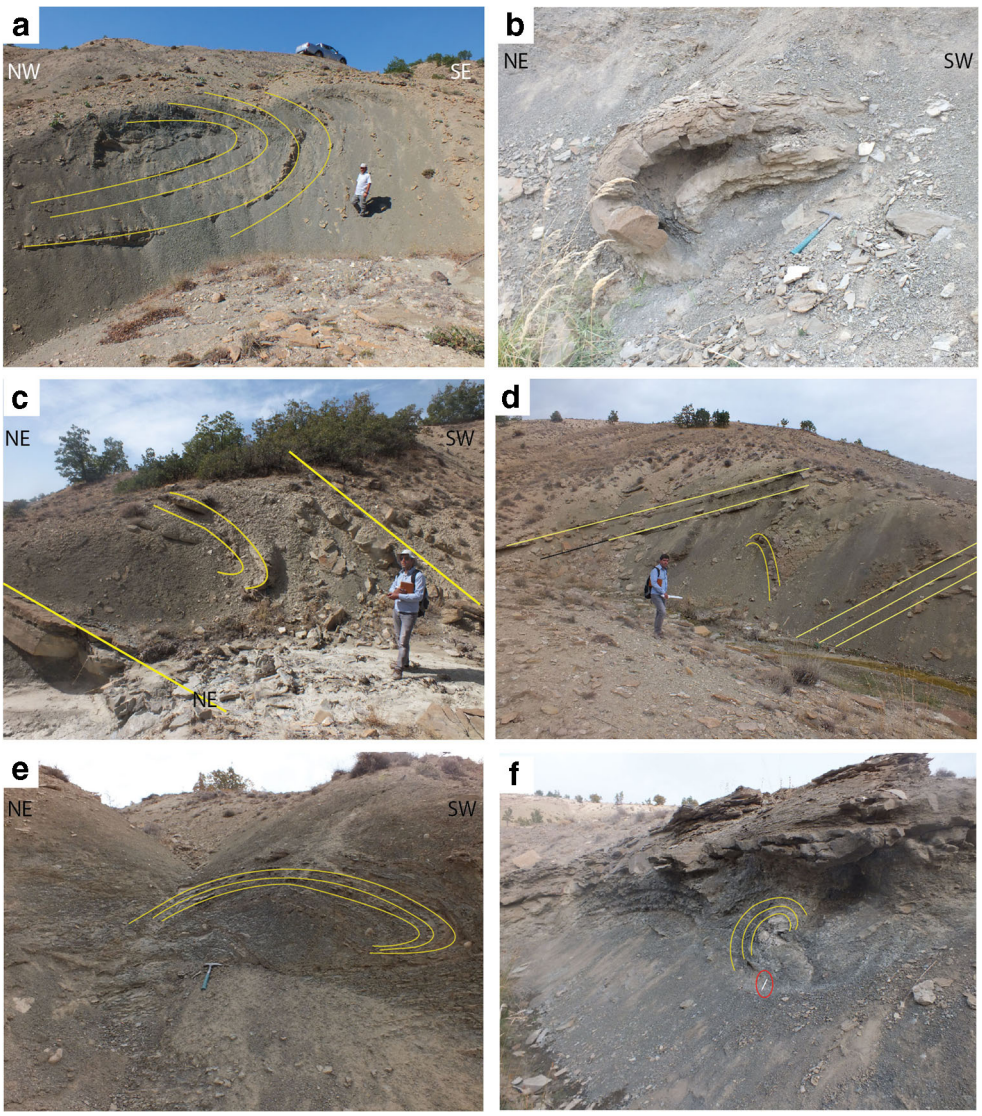

Fig. 8 Slumps. **a** Large-scale slump sheets involving interbedded sandstone and marl (section 1 in Fig. 7). **b**–**d** Relatively small-scale slump sheets observed on interbedded sandstone and marl. **e** Slump folds observed within the marl facies. **f** Small-scale slump folds observed in mud matrix-supported conglomerates

folds tend to develop in lithologies more susceptible to ductile deformation. In unconsolidated sediments, large-scale slump masses may be derived from the shelf edge or upper slope. This interpretation shows that the gravity effect is important in the formation of these structures in the study area.

Load casts

Description: Load casts are common in the deep-marine deposits of the Kırkgeçit Formation. They are developed in several facies: sandstone-marl, alternations, coarse-grained sandstone-fine-grained sandstone alternations and medium-grained sandstone-fine-grained sandstone alternations. (Figs. 9c–f and 10). Deformed beds with load casts are overlain and underlain by undeformed beds. These structures have continuity in the lateral direction (approximately 10 m). They represent both simple and pendulous load-cast varieties. Simple load casts with half-spherical forms are one of the commonly observed structures. Pendulous load casts occur in fine-grained sandstones underlying coarse-grained sandstones that are interconnected (Fig. 10f). Their dimensions vary from 3 to 15 cm, and their geometry varies from symmetric, asymmetric to irregular. They can show internal lamination. The load casts are generally associated with flame structures.

Interpretation: The base of beds becomes deformed due to gravity-related stability, the density difference between the layers and as a result of liquefaction (Anketell et al. 1970; Owen 1987; Moretti et al. 1999). The bottom part of the upper layer tends to sink into the underlying bed in the form of rounded levels, and load casts are formed. The morphological features of the load casts depend on the dynamic viscosity ratio of the liquefied sediment layers (Mills 1983; Alfaro

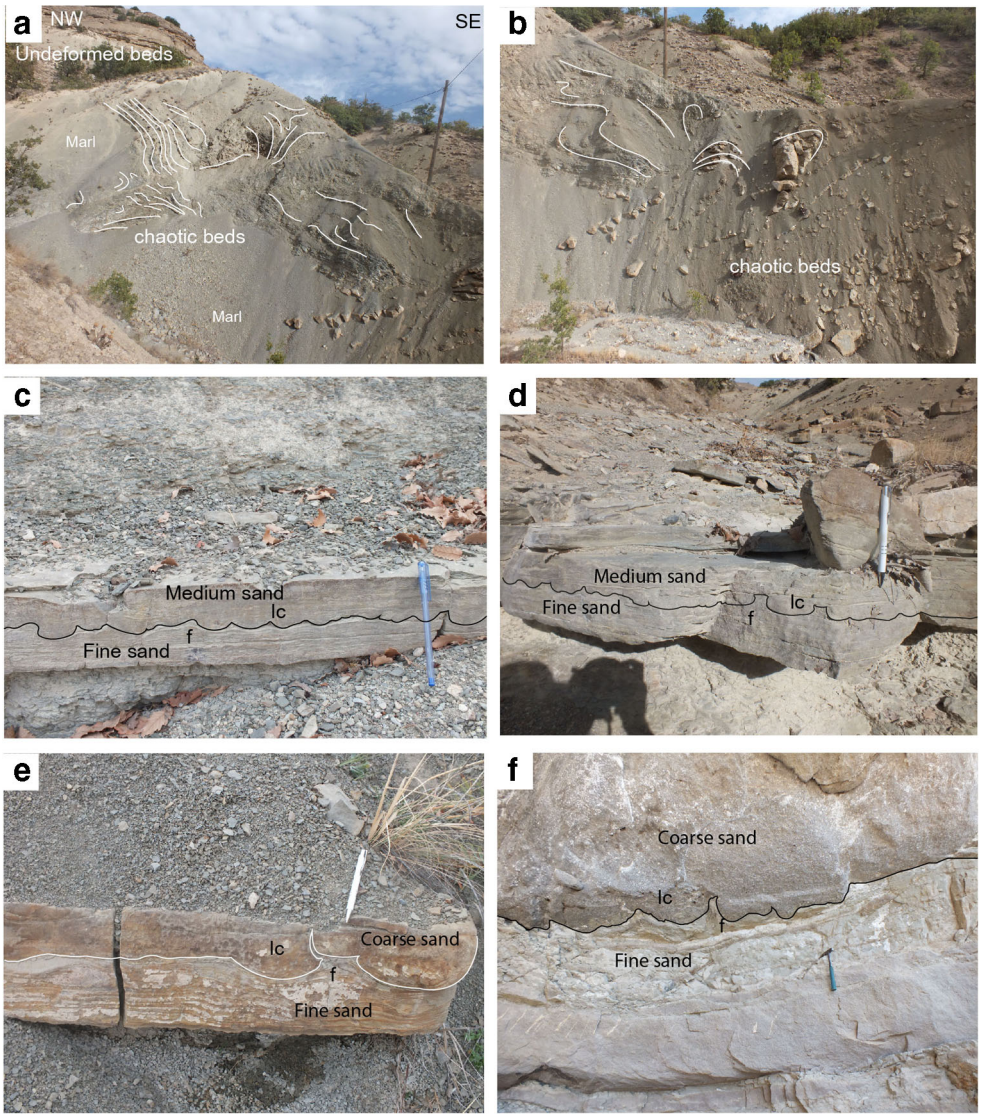

Fig. 9 **a**, **b** Chaotic strata. **c**–**f** Load casts and flame structures at the interface between fine sandstone and coarse sandstone

et al. 1997) and the duration of the liquefaction phase (Owen 2003; Alves 2015).

Flame structures

Description: Flame structures are usually observed with load casts (Fig. 10), and their sizes vary from 3 cm to 1 m. They are one of the structures widely observed in the study area. Flame structures have both large-scale and small-scale varieties. Large-scale flame structures affect areas of 1–2 m in the lateral and vertical directions. They present regular, cusp and dome morphologies.

Interpretation: The upward movement of sediment in response to density instabilities involves either hydroplastic or liquefied flow. The dynamic viscosity of the underlying marls is lower than that of the overlying sands (Anketell et al. 1970), and consequently, the diapiric intrusion of fine-grained sediments forms flame structures (Mills 1983).

Convolute lamination

Description: Convolute laminae consist of curved and deformed laminae (Fig. 11a–e) with laterally alternating convex and concave morphologies, limited at top and bottom by undeformed layers. The widths of the convex laminae are between 5 and 20 cm, and the heights are between 10 and 20 cm. Their lateral continuity reaches tens of metres. Different morphological types of convolute laminations are defined, such as overturned folds, mushroom-shaped folds and diapir folds. They generally affect stratified, fine- to medium-grained sands (Fac. 4). Convolute laminations are generally observed in a thin single layer, sometimes at the upper level of a thick layer and are rarely observed with the B and AB sections of the Bouma sequence.

Interpretation: Convolute lamination develops when sediment masses are exposed to hydroplastic deformation. They are formed by liquefaction rather than fluidization of water

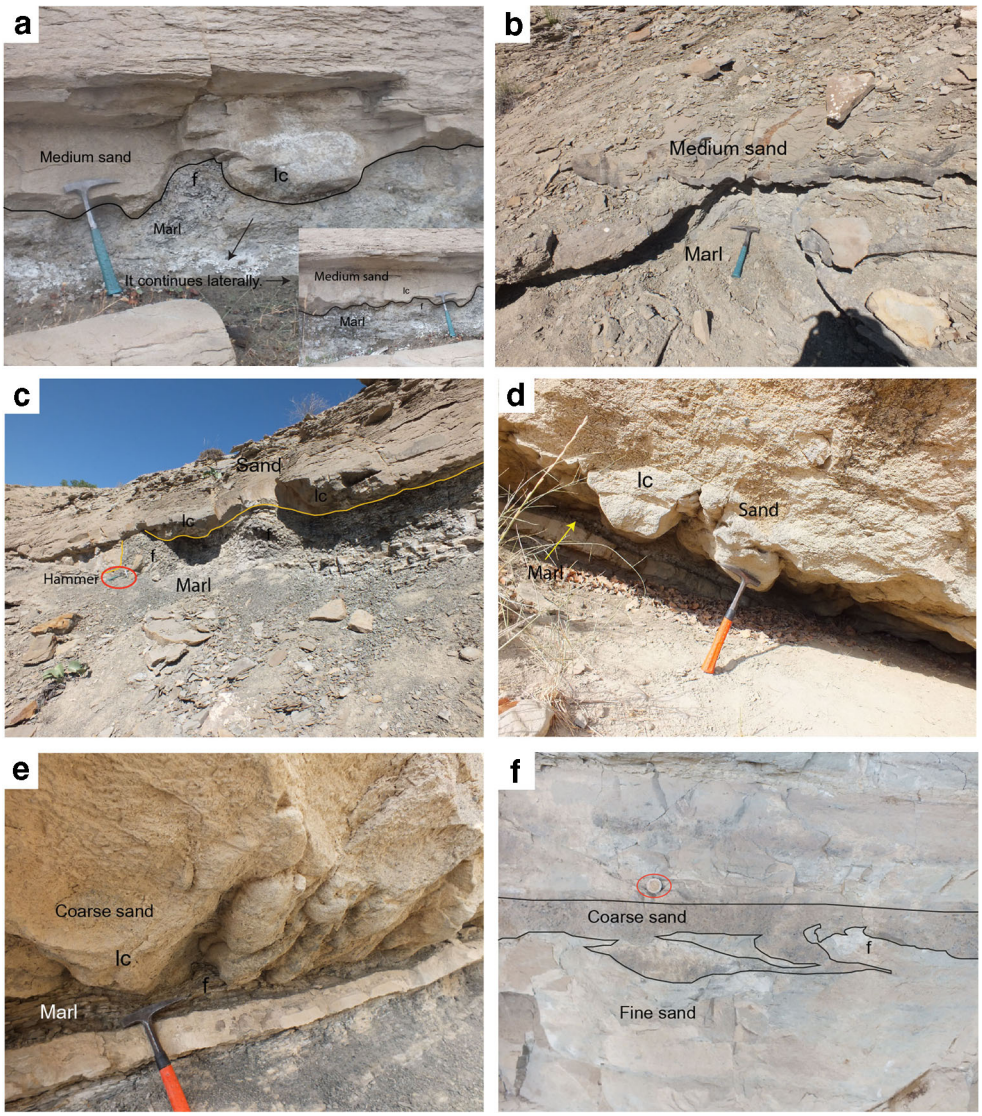

Fig. 10 **a**–**e** Load casts and flame structures at the sandstone and marl interface. **f** Interconnected pendulous load casts that occur in fine-grained sandstones underlying coarse-grained sandstones

(Lowe 1975). Similar features have been described in the literature (e.g., Kuenen 1953; Anketell et al. 1970; Visher and Cunningham 1981; Hempton and Dewey 1983; Mills 1983). The progressive growth of convolute folds depends on the continuity of sedimentation and the movement of water (Lowe 1975).

Clastic dykes

Description: Clastic dykes are present in the marl facies and are observed in a few locations in the study area (Fig. 11f). The size of the dykes is up to 50 cm, and the thicknesses are 3–4 cm. These dykes are observed at the lower level of the facies with lenticular geometry composed of sandstones.

Interpretation: Such structures develop as a result of intrusion into associated facies of liquefied and fluidized unconsolidated, cohesionless material (Lowe 1975). Sandstone dykes in this study may occur under aseismic conditions as a result of the deposition of dense sand flows in pelagic environments (e.g. Beaudoin and Friès 1982; Beaudoin et al. 1983). This flow involves the intrusion of material into surrounding beds. These structures are described as rupture structures (e.g. Davies 1965).

Water-escape structures

Description: Water-escape structures are local and consist of disrupted laminations (Fig. 12a) observed in the upper levels of the stratified sandstone layers (Fac. 4). There are also levels in which syn-sedimentary faults are observed (Fig. 12b).

Interpretation: These structures are similar to the internal cusps described by Owen (1995). The formation of such structures is related to the upward movement of water and vertical shear stress (Owen 1987). They represent local zones where the water moves.

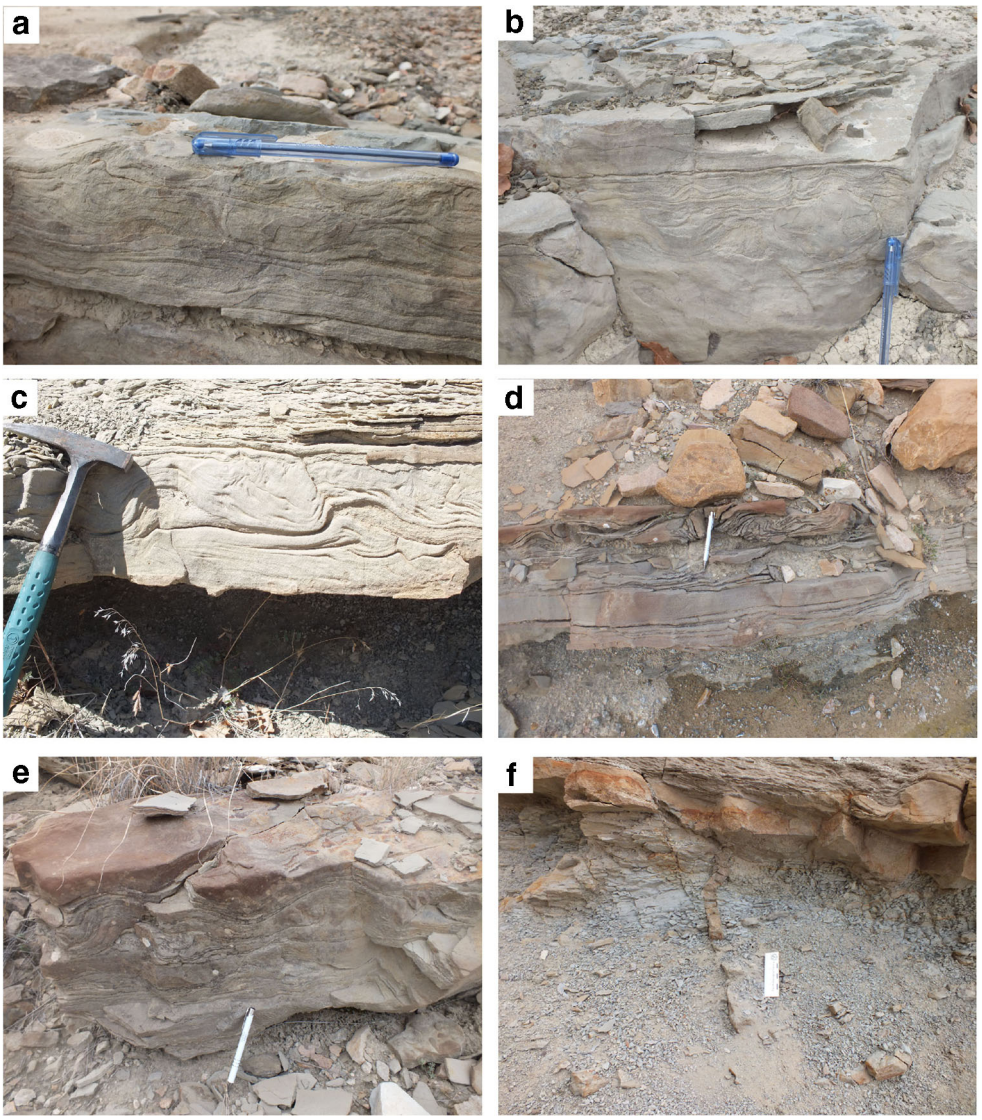

Fig. 11 **a**–**e** Convolute laminations observed on fine grained sandstone. **f** Sand dyke developed in marl facies

Syn-sedimentary faults

Description: These faults are generally observed as high-angle normal syn-sedimentary faults. The offset of normal faults ranges from 2 to 50 cm (Fig. 12b–f). Syn-sedimentary faults affect sandstone and marl facies. In some locations, the faults consist of a series of faults with small offsets in a single layer (Fig. 12b). Faults affecting mostly several layers are observed at several levels.

Interpretation: When the porewater pressure increases in soft sediments, brittle deformation occurs if this pressure is not strong enough to liquefy the sediment (Owen 1987; Vanneste et al. 1999). Brittle deformation is related to the cohesive behaviour of rocks. More consolidated and less water-saturated sediments exhibit brittle behaviour (e.g., Rossetti 1999; Rossetti and Goes 2000).

Discussion

Palaeoenvironmental interpretation of the study area

A classic submarine fan system was not developed in the study area, and a turbidite sequence with the aforementioned characteristics, for example all parts or part of the bouma sequence, rarely occurred; this type of turbidite is precipitated by low-density currents. Although these currents are observed in the middle and distal parts of the basin, such currents can occur in any part of the system (shelf edge, slope and basin) (e.g. Mulder and Alexander 2001). Kneller and Branney (1995) used the term 'sustained high-density currents' to explain the deposition of thick massive beds. Lowe (1982) considered the coarse-grained beds to have a distinctly different character from Bouma sequences and attributed them to 'high-density turbidity currents'. The massive and stratified sandstones identified in this study may indicate the presence of high-density turbidite flows. Channel deposits consisting of sand matrix-supported conglomerates, massive and stratified sandstones with different sizes and lithologies developed. Similar features to the facies defined in the study area has been recognized in SE Crete (Alves and Lourenço 2010; Alves and Cupkoviç 2018), which is an example of extensional basins at an active continental margin. According to Alves and Lourenço (2010) and Alves and Cupkoviç (2018), the excess of coarse-grained sediments in deep-water systems implies that the sea floor is unstable and represents environments where the slope of the layers increases with tectonic effects.

In the study case, the movement directions of slump folds and the imbrication of conglomerates demonstrate that the palaeo-slope direction of the Kırkgeçit Basin was south-southwest. The presence of slump sheets and sediments deposited from high-density turbidite flows and high mud ratios reflect a marl-rich slope environment. These slope deposits are covered by the prograding shelf sands (calcarenites) of the Bozaltı member (Figs. 3 and 4).

Deformation trigger mechanisms

The studied successions were deposited in deep marine basins located in tectonically active back-arc settings. Soft-sediment deformation structures observed in deep-sea environments have various triggering mechanisms. The different triggering mechanisms controlling the generation of the studied soft-sediment deformation structures are considered and discussed below.

Deformation due to rapid sedimentation and overloading

Although the slow accumulation of sediment results in stable sedimentation, naturally occurring traps within the sediment accelerate sedimentation locally and cause less stable sediments (Moore 1961). More likely, thicker layers are associated with higher sedimentation rates. Slump folds described in this study are generally observed in areas where thin-bedded sandstones and marls are intercalated.

The absence of convolute laminations in very thick layers can eliminate the triggering mechanism due to rapid sedimentation in their formation.

Liquefaction mechanisms can be triggered by a variety of factors, including seismic tremors, storm waves or periodic pressure changes associated with wave breaks and rapid sedimentation. Many types of soft-sediment deformation structures, including load structures, convolute laminations and water-escape structures, are widely observed in turbidite deposits (Lowe 1975; Allen and Banks 1972; Stromberg and Bluck 1998; Moretti et al. 2001; Tinterri et al. 2016). Most of these structures occur in association with the liquefaction and fluidization of water-saturated sediment (Allen 1977), which are associated with high sedimentation rates, after exceeding the lower limit of stability of the sediment due to rapidly increased thickness (Moretti et al. 2001). Load casts (simple, pendulous and asymmetric) with various characteristics can occur depending on the loading event resulting from rapid sedimentation in relation to liquefaction and local fluidization (Anketell et al. 1969; Moretti et al. 2001).

Sand flows filling open cracks in the seabed or sand injected into unconsolidated marl sediments occur by overloading the sediment (Montenat et al. 2007). Occasional vertical cracks may develop on semi-compacted sedimentary surfaces. These cracks are filled with subsequent sand flows. The dykes identified in this study may have been formed in this way.

Deformation due to slopes

One of the most likely causes of slump movement in an uncompressed sediment mass is an increase in the slope inclination. The increase in this angle may occur due to deposition and tectonic movements or as a result of erosion from the bottom due to turbidite currents (Morgenstern 1967).

Although steep slopes are necessary for the formation of slump folds, such folds may also occur on gentle slopes as low as 1° (Dill 1964; Mills 1983). Factors affecting the formation of slump structures on gentle slopes are sediment type, sedimentation rate and water depth. Morgenstern (1967) described slump structures on the slopes of a prodelta with a slope of 4°. Previous researchers stated that sediments exposed to slump movements on slopes reacted to three main triggering mechanisms: (1) high sedimentation rate or sediment loading, (2) the presence of steep slopes or (3) seismic trigger mechanisms (Naylor 1981). The stability of sediments deposited on a slope depends on the shear stress of the sediments, the rate of burial and the rate of increase of this stress. These factors are controlled by, for example, grain size distribution, homogeneity, sediment accumulation rate, degree of consolidation and porewater pressure (Moore 1961). However, the magnitude of the shear stress increases with the slope angle and with the density and thickness of the overlying sediment on the continental slopes (Lewis 1971; García-Tortosa et al. 2011). The sediment masses in a basin slope setting are frequently unstable, and the downward movement is initiated by tectonic and seismic movements (e.g. Yang and van Loon 2016; Alves and Lourenço 2010; Alves 2015). As a result, slides and slumps can be related to steep slopes with or without earthquakes. However, the presence of a slope with a high gradient alone is not sufficient for developing slump sheets. No asymmetry in the forms of flame structures and convolute laminations in the study area (e.g. Oliveira et al. 2009; Gladstone

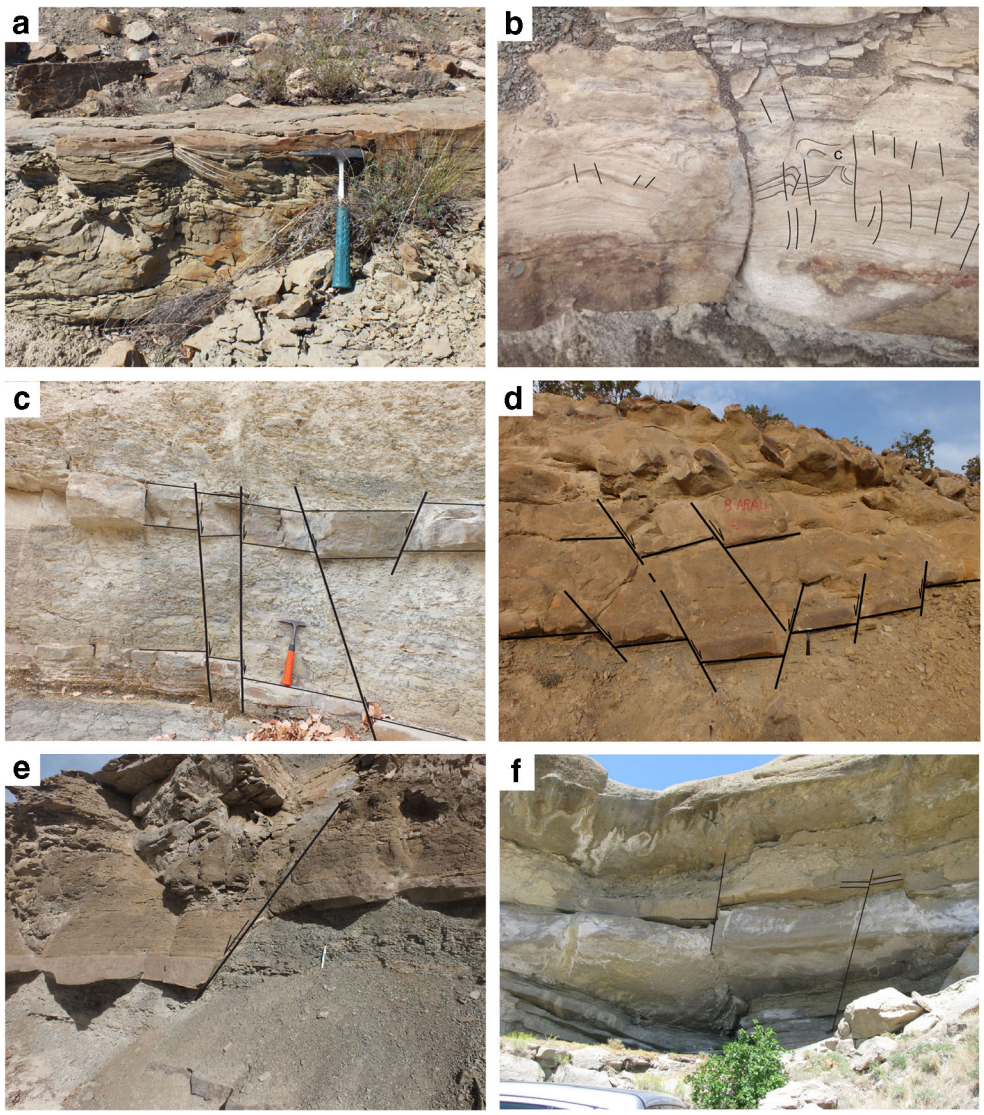

Fig. 12 **a** Water-escape structure. **b** Syn-sedimentary faults observed in fine-grained sandstone and associated water-escape structures (c : cusps). **c-f** Syn-sedimentary faults associated with sandstones and marls

et al. 2018) demonstrate a lack of slope effect and downslope shear for the formation of these structures.

Deformation due to turbidity currents

Turbidity currents are often associated with slump structures. The facies are usually carried from shallow to deep; that is, the sediment load on the slope is activated by gravity (King 1994; Collinson et al. 2006). Slides and slumps developed in liquefied sediments can occur on a slope of up to 3° (Bridge and Demicco 2008). Slumps and curved laminae are formed in the sediments where slope reduction causes deceleration. The presence of the slope described in the study area may indicate that small-scale slump sheets developed as a result of turbidity currents. However, very large-scale slump masses (Fig. 6a) cannot be associated with such currents.

Convolute laminations are observed both in marine environments (Tinterri et al. 2016; Gladstone et al. 2018) and in terrestrial environments (Koç-Taşgın and Türkmen 2009). It is stated that the formation of convolute laminations in turbidite deposits is related to flows of density/turbidity currents (e.g. Lowe 1982; Pickering et al. 1986). The full series of the Bouma sequence, which characterizes low-density turbidites, is rarely observed in the study area. Such structures are not formed by the presence of high-density currents. The characteristics of convolute bedding within the Moroccan turbidite system, offshore north-western Africa, have been compared with the characteristics of 'convolute bedding' in the Aberystwyth Grits as defined by Kuenen (1953), by Gladstone et al. (2018). In convolute laminations (e.g. the Aberystwyth Grits) defined in turbidite sequences, the silt and mud ratio increases towards the upper part of the convolution layer and has a dark colour upward. However, such a colour and grain size change are not observed in convolute laminations defined in the study area. In addition, ripple cross-laminated sands formed in the lower levels of the convolute laminae by turbidity currents (Kuenen 1953; McClelland et al. 2011; Gladstone et al. 2018) are not observed in the samples in this study. Structures with an optimal thickness of 2–10 cm occur in turbidite deposits developed between the Bouma B and D divisions. In the study area, the thickness of the convolute laminations is generally more than 10 cm and is not observed with A and D, the sections of the Bouma sequence.

However, it should be noted that the mechanism leading to the formation of turbidity currents is often but not always associated with seismic activity and tsunami movements (e.g. Schnellmann et al. 2002; Arai et al. 2013).

Deformation due to tsunamis

Tsunami deposits have been reported in various geological environments, ranging from shallow sea (Atwater and Moore 1992; Papadopoulos et al. 1994; Bondevik et al. 1997; Meshram et al. 2011) to deep sea (Kastens and Cita 1981). However, many deformation structures (load casts, flame structures, clastic dykes and homogenites) have been identified as a result of tsunamis (Cita and Aloisi 2000; Shiki and Cita 2008). The liquefaction developed in sandy material by tsunamis can result in the formation of complex convolutions and load structures (Obermeier 1996; Obermeier and Pond 1999). Consequently, tsunamis can have significant depositional and erosional impacts on coastal sedimentation (Dawson et al. 1991; Dawson 1994; Dawson and Shi 2000; Smith et al. 2007) rather than deep-sea deposition. It should also be noted that tsunami movements have a seismic trigger mechanism.

Deformation due to tectonism and seismic activity

The development of debris flows and slump folds observed along estuary benches in the estuary deposits associated with fluvial sediments are associated with seismic activity (Rossetti and Santos 2003). On the Calabrian ridge (southern Italy), Kastens (1984) stated that the mechanism causing the formation of sediment flow and turbidity deposits is seismic activity and mentioned that the sediment transport process in the basin slopes first starts with a rotational slump movement and then continues in the form of debris flows and intense currents. The olistolithic blocks indicate that the mechanism that initiated the deformation was related to tectonic and seismic movements. In particular, the basin shows faulting features at the base that facilitate the formation and settlement of olistoliths (Fig. 13a, b). The blocks are often associated with unstable slope events triggered by major tectonic phases. Most of these major tectonic phases are associated with significant uplift and exposure of the upper crust and subsequent erosion (Dunlap et al. 2013; Alves 2015). Alves and Cupkoviç (2018) defined slump structures developing as a result of the increase in the slopes of the strata due to the active normal faulting in SE Crete, an extensional basin on the continent. The SE Crete extensional basin is similar to the Elazığ Basin which has tectonic conditions in a back-arc basin at the active continental edge (Fig. 2).

Faulting at the basin base is one of the possible reasons for the formation of slump sheets (e.g. Kuenen 1967; Corbett 1973; Debacker et al. 2001). Seismic activity accompanying these faults can be the triggering mechanism that initiates the sliding motion (e.g. Corbett 1973; Kastens 1984). However, tectonics can induce tilting without seismic shocks. Slump folds are one of the many structures that can occur in unconsolidated sediments under the influence of seismic activity. In the northern part of the study area (Hacıtemur area) (Koç-Taşgın 2018; Koç-Taşgın and Altun 2019) and in different locations of the same unit in the Elazığ Basin, the presence of seismically induced slumps (Fig. 13c) and soft-sediment deformation structures (Neptunian dykes) (Koç-Taşgın 2018) have been related to extensional movements. Different lithologies

may display diverse mechanical behaviours; for example, folding develops in lithologies that are more susceptible to plastic deformation, while thrusts may form in lithologies that are more prone to brittle styles of deformation (Alsop and Marco 2011). The syn-sedimentary faults that change their main offset rate upwards and that disappear in the upward and downward directions are related to seismic shocks and are of syn-sedimentary origin (Seilacher 1969, 1984). The development of such syn-sedimentary faults is associated with localized stress conditions within the layers induced by seismicity.

Many examples of chaotic deposits have been described in current and old deep-water settings (Doyle and Pilkey 1979; Watkins et al. 1979; Saxov and Nieuwenhuis 1982; Pickering et al. 1986). Such structures are sliding and slumping sediments that exceed slip resistance and are induced by gravity effects. In addition, sediment movements can be induced by earthquakes and/or shocks generated by tsunamis, and chaotic strata may occur (Doyle and Pilkey 1979; Watkins et al. 1979; Pickering 1982, 1986; Bally 1983; Pickering et al. 1986). Montenat et al. (2007) interpreted that similar structures were formed as a result of the liquefaction of large volumes of sediments due to seismic activity.

In addition, pillar-dish structures, sill and convolute lamination structures defined in deep-sea turbidite deposits are associated with seismic activity (e.g. Valente et al. 2014). Water-escape structures and dykes are related to fluidization. The limitation of convolute laminations by undeformed layers strengthens the hypothesis that the formation of these structures was related to seismic activity. Seismic activity is a natural phenomenon associated with active tectonic movements. Contemporary seismic activity includes regional extensional moving belts such as continental opening zones (e.g. East African Rift) and SE Crete (Alves 2015). The geological records of past seismic activity have been preserved in sedimentary rocks and are defined as seismites. Seismites are particularly common in tectonically active regions such as back-arc basins (e.g. Bryan et al. 2001). Sims (1975) emphasized that each seismic deformation horizon is formed by seismic activity of 6 or greater. Marco and Agnon (1995) calculated a magnitude over 4.5 for starting liquefaction. Morgenstern (1967) argued that there may be a correlation between large-scale slump sheets associated with submarine sediments and nearby earthquakes with large magnitudes. In the Alkyonides Basin, a mass related to submarine slumping was determined, and the conclusions was that the mechanism triggering this mass flow was the first seismic shock in Greece in 1881 with magnitude between 6.4 and 6.7 (Perissoratis et al. 1984). The magnitudes of all seismic activity described by the researcher are greater than 6 and emphasize that slumps may occur on slopes with a gradient of less than 3° in relation to seismic activity of such magnitude.

Especially the presence of slumps indicates that seismic activity with magnitudes of 6 or more might have occurred in this region.

Conclusions

The Seherdağı member of the middle Eocene-Oligocene Kırkgeçit Formation includes six facies (sand matrix-

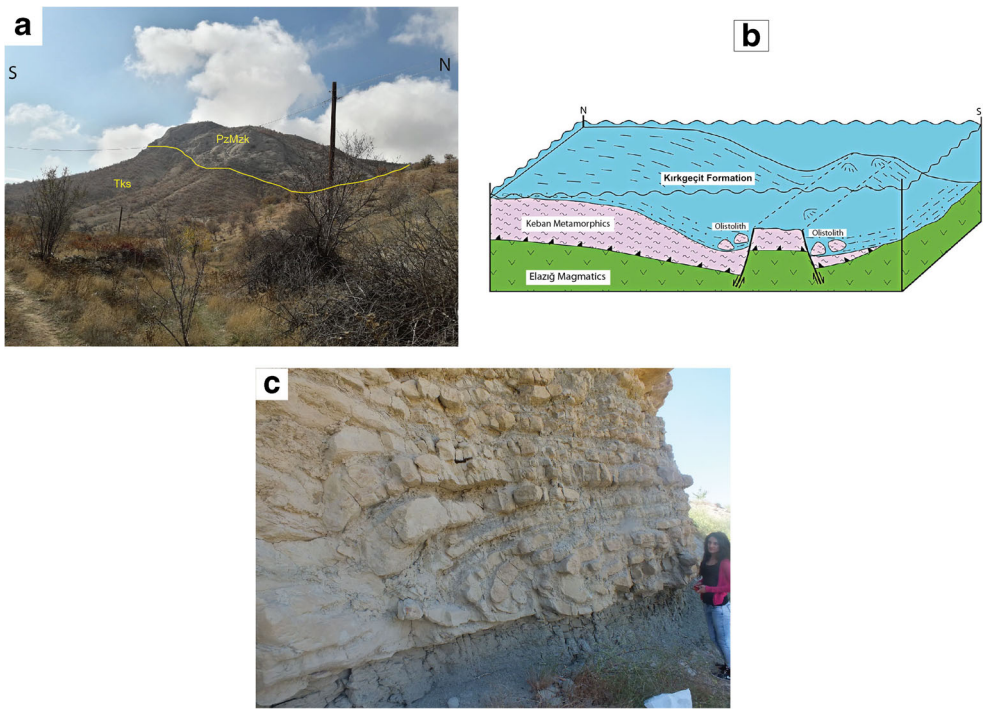

Fig. 13 **a** The olistolith block (Keban metamorphic rocks; PzMzK) observed in the Seherdağı member (Tks) of the Kırkgeçit Formation. **b** Block diagram showing the formation of olistoliths in the study area (modified form Aksoy and Turan 1997). **c** Slump folds observed in the alternation of calcarenite-carbonate mudstone in the northern part (up to 6 km) of the study area (Koç-Taşgın and Altun 2019)

supported conglomerates, mud matrix-supported conglomerates, massive sandstones, stratified sandstones, graded sandstones and marls) that represent a mud-rich submarine slope environment containing a complex channel system. Soft-sediment deformation structures are frequent and include slump folds, chaotic strata, load casts, flame structures, water-escape structures, convolute laminations, clastic dykes and syn-sedimentary faults. The deformation mechanisms and important factors of the structures are slope gradient, density difference, liquefaction and fluidization. The main mechanism triggering deformation structures was tectonic and seismic movements.

The Kırkgeçit Formation is a unit consisting of marine sediments that developed due to the extensional regime in a back-arc basin behind a supra-subduction zone (the Arabian Plate, which subducts beneath the Eurasian Plate) in the Elazığ Basin. In addition, the presence of olistoliths derived from older units within the lowermost part of the unit is a sign that the basin base has a block fault structure. Therefore, tectonism and seismic activity resulting from tectonic movements are important triggering mechanisms for the formation of soft-sediment deformation structures. As a result of the evaluation of the data, seismic events with intensities of at least 6 or more are determined to have occurred in the region.

The present study can provide a guide for the investigation of similar soft-sediment deformation structures in the marine sediments in the Elazığ and eastern Anatolia regions, as well as in the overlaying units.

Acknowledgements Thanks to my colleague Ezher TAGLIASACCHI for English editing. We would like to thank the reviewers and editor who made constructive suggestions and contributions. This article is produced from Fırat ALTUN's master's thesis, which I supervised.

Funding information The Scientific and Technical Research Council of Turkey (TUBITAK) provided funding for this study (Project no. 116Y017).

References

Aalto KR (1976) Sedimentology of melange; Franciscan of Trinidad, California. J Sediment Petrol 46:913–929

Aksoy E, Turan M (1997). Van ve Elazığ yörelerinde Kırkgeçit Formasyonundaki olistolit yerleşimlerinin tektonik önemi. Selçuk Üniv Mim Fak 20.Yıl Jeoloji Semp Bildiriler 35-44

Aksoy E, Türkmen İ, Turan M (2005) Tectonics and sedimentation in convergent margin basins: an example from the Tertiary Elazığ basin, Eastern Turkey. J Asian Earth Sci 25:459–472

Alfaro P, Moretti M, Soria JM (1997) Soft-sediment deformation structures induced by earthquakes (seismites) in Pliocene lacustrine deposits (Guadix-Baza Basin, Central Betic Cordillera). Eclogae Geol Helv 90:531–540

Allen JRL (1977) The possible mechanics of convolute lamination in graded sand beds. J Geol Soc 134:19–31

Allen JRL, Banks NL (1972) An interpretation and analysis of recumbent-folded deformed cross-bedding. Sedimentology 19: 257–283

Alsop GI, Marco S (2011) Soft-sediment deformation within seismogenic slumps of the Dead Sea basin. J Struct Geol 33:433–457

Altun F (2018) Kırkgeçit Formasyonu'nda (Elazığ Batısı) Gözlenen Yumuşak Çökel Deformasyon Yapılarının Özellikleri ve Oluşumu. Yüksek Lisans Tezi, Fırat Üniv Fen Bli Enst 94s

Alves TM (2015) Submarine slide blocks and associated soft-sediment deformation in deep-water basins: a review. Mar Pet Geol 67:262–285

Alves TM, Cupkoviç T (2018) Footwall degradation styles and associated sedimentary facies distribution in SE Crete: insights into tilt-block extensional basins on continental margins. Sediment Geol 367:1–19

Alves TM, Lourenço SDN (2010) Geomorphologic features related to gravitational collapse: submarine landsliding to lateral spreading on a Late Miocene–Quaternary slope (SE Crete, eastern Mediterranean). Geomorphology 123:13–33

Alves TM, Lykousis V, Sakellariou D, Alexandri S, Nomikou P (2007) Constraining the origin and evolution of confined turbidite systems: southern Cretan margin, Eastern Mediterranean Sea (34°30–36°N). Geo-Mar Lett 27:41–61

Anketell JM, Cegła J, Dżułyński S (1969) Unconformable surfaces formed in the absence of current erosion. Geol Roman 8:41–46

Anketell JM, Cegla J, Dzulinsky S (1970) On the deformational structures in systems with reversed density gradients. Ann Soc Geol Pol 1 (XL). 3–30

Arai K, Naruse H, Miura R, Kawamura K, Hino R, Ito Y, Inazu D, Yokokawa M, Izumi N, Murayama M, Kasaya T (2013) Tsunami-generated turbidity current of the 2011 Tohoku-Oki earthquake. Geology 41(11):1195–1198

Atwater BF, Moore AL (1992) A tsunami about 1000 years ago in Puget Sound, Washington. Science 258(5088):1614–1617

Bally AW (Editor) (1983) Seismic expression of structural styles. Am Assoc Petrol Geol Studies in Geology Ser 15: 1,2,3

Basilone L, Lena G, Gasparo-Morticelli M (2014) Synsedimentary tectonic, soft-sediment deformation and volcanism in the rifted Tethyan margin from the Upper Triassic–Middle Jurassic deep-water carbonates in Central Sicily. Sediment Geol 308:63–79

Beaudoin B, Friès G (1982) Filons gréseux sédimentaires, per descensum, dans un système de fractures ouvertes. Le cas de l'Albien de Bevons (Alpes-de-Haute-Provence) C. R. Acad. Sci., Paris 295: 285-387

Beaudoin B, Friès G, Joseph P, Paternoster B (1983) Sills gréseux sédimentaires injectés dans l'Aptien supérieur de Rosans (Drôme). C. R. Acad Sci Paris 296:387-392

Bhattacharya HN, Bandyopadhyay S (1998) Seismites in a Proterozoic tidal succession, Singhbhum, Bihar, India. Sediment Geol 119:239–252

Bhattacharya HN, Bhattacharya B (2010) Soft-sediment deformation structures from an ice-marginal storm–tide interactive system, Permo-Carboniferous Talchir Formation, Talchir Coalbasin, India. Sediment Geol 223:380–389

Bingöl AF (1984) Geology of the Elazığ area in the Eastern Taurus region. International Sympozium on the geology of the Taurus Belt, O.Tekeli and M.C. Göncüoğlu (eds) Proceedings, Ankara, 209-216

Bondevik S, Svendsen JI, Mangerud J (1997) Tsunami sedimentary facies deposited by the Storegga tsunami in shallow marine basins and coastal lakes, western Norway. Sedimentology 44:1115–1131

Bridge J, Demicco R (2008) Earth surface processes, landforms and sediment deposits. Cambridge University Press, Cambridge

Brogi A, Capezzuoli E, Moretti M, Olvera-García E, Matera PF, Garduno-Monroy VH, Mancini A (2018) Earthquake-triggered

soft-sediment deformation structures (seismites) in travertine deposits. Tectonophysics 745:349–365
Bryan SE, Holcombe RJ, Fielding CR (2001) Yarrol terrane of the northern New England Fold Belt: forearc or backarc?. Austral Jour Earth Sci 48:293–316
Chen J, Lee HS (2013) Soft-Sediment deformation structures in Cambrian siliciclastic and carbonate storm deposits (Shandong Province, China): differential liquefaction and fluidization triggered by storm-wave loading. Sediment Geol 288:81–94
Cita MB, Aloisi G (2000) Deep-sea tsunami deposits triggered by the explosion of Santorini (3500 y BP) eastern Mediterranean. Shiki T, Cita MB and Gorsline DS (eds.), Sedimentary Features of Seismites, Seismo-turbidites and Tsunamites. Sediment Geol 135: 181–203
Collinson JD, Mountney NP, Thompson DB (2006) Sedimentary structures, Third Edition. Terra Publishing, Harpenden
Corbett KD (1973) Open cast slump sheets and their relationship to sandstone beds in an Upper Cambrian flysch sequence, Tasmania. J Sediment Petrol 43:147–159
Cremer M, Stow DAV (1986) Sedimentary structures of finegrained sediments from the Mississippi fan: thin-section analysis. In: Bouma, A. H., Coleman, J. M., et al., (Eds) Init. Repts. DSDP, 96: Washington (U.S. Govt. Printing Office), 519-532
Cronin BT, Çelik H, Hurst A, Türkmen İ (2005) Mud prone entrenched deep-water slope channel complexes from the Eocene of eastern Turkey, In: D.M. Hodgson and S.S. Flint, (Eds), Submarine Slope Systems: Processes and Products, Geological Society, London, Special Publications 244: 155-180
Davies HG (1965) Convolute lamination and other structures from the lower coal measures of Yorkshire. Sedimentology 5:305–325
Dawson AG (1994) Geomorphological processes associated with tsunami runup and backwash. Geomorphology 38:83–94
Dawson AG, Shi S (2000) Tsunami deposits. Pure Appl Geophys 157: 187–897
Dawson AG, Foster IDL, Shi S, Smith DE, Long D (1991) The identification of tsunami deposits in coastal sediment sequences. Sci Tsun Haz 9(1):73–82
Debacker TN, Sintubin M, Verniers J (2001) Large-scale slumping deduced from structural and sedimentary features in the Lower Palaeozoic Anglo-Brabant fold belt, Belgium. J Geol Soc 158: 341–352
Dewey JF, Hempton MR, Kidd WSF, Şengör AMC (1986) Shortening of continental litosphere: the neotectonics of Eastern Anatolia a young collision zone, In: Coward, M.P., Reis, A.C. (Eds.), Collision Tectonics. Geological Society of America Bulletin Special Publication 19: 3–36
Dill RF (1964) Sedimentation and erosion in Scripps Submarine Canyon Head. In: Papers in Marine Geology (Ed. by R. L. Miller), pp. 23-41. Macmillan, New York
Doyle LJ, Pilkey OH (Editors) (1979) Geology of continental slopes. Soc Econ Paleontol Min Spec Pub 27: 374 pp
Dunlap DB, Wood LJ, Moscardelli LG (2013) Seismic geomorphology of early North Atlantic sediment waves, offshore northwest Africa. Interpretation 1:SA75–SA91
Gamboa D, Alves TM (2015) Three-dimensional fault meshes and multilayer shear in mass-transportblocks: Implications for fluid flow on continental margins. Tectonophysics 647-648:21–32
García-Tortosa FJ, Pedro Alfaro P, Gibert L, Scott G (2011) Seismically induced slump on an extremely gentle slope (1°) of the Pleistocene Tecopa paleolake (California). Geology 39:1055–1058
Ge Y, Zhong J (2017) Trigger recognition of Early Cretaceous soft-sediment deformation structures in a deep-water slope-failure system. Geol J. 1-16
Gibert L, Sanz de Galdeano C, Alfaro P, Scott G, López Garrido AC (2005) Seismic induced slump in Early Pleistocene deltaic deposits of the Baza Basin (SE Spain). Sediment Geol 179:279–294
Gladstone C, McClelland HLO, Woodcock NH, Pritchard D, Hunt JE (2018) The formation of convolute lamination in mud-rich turbidites. Sedimentology 65:1800–1825
Greb S, Archer AW (2007) Soft-sediment deformation produced by tides in a meizoseismic area, Turnagain Arm, Alaska. Geology 35(5): 435–438
Hein FJ (1982) Depositional mechanisms of deep sea coarse clastic sediments, Cap Enrage Formation, Quebec. Can Jour Earth Sci 19:267–287
Hempton MR (1985) Structure and deformıation history of the Bitlis Suture near Lake Hazar, SE Turkey. Geol Soc Am Bull 96:223–243
Hempton RM (1987) Contraints on Arabian plate motion and extensional history of the Red Sea. Tectonics 6(6):687–705
Hempton MR, Dewey JS (1983) Earthquake-induced deformational structures in young lacustrine sediments, East Anatolian Fault, southeast Turkey. Tectonophysics 98:T14–T17
Hiscott RN, Middleton GV (1979) Depositional mechanics of thick-bedded sandstones at the base of a submarine slope, Tourelle Formation (Lower Ordovician), Quebec, Canada. Soc Econ Paleontol Min Spec Pub 27:307–326
Hubert C, Lajoie J, Eonard MA (1970) Deep sea sediments in the Lower Palaeozoic Quebec Supergroup. Geol Assoc Can Spec Pub 7:103–125
Johnson HD (1977) Sedimentation and water escape structures in some late Precambrian shallow marine sandstones from Finmark, North Norway. Sedimentology **24**:389–411
Jones AP, Omoto K (2000) Towards establishing criteria for identifying trigger mechanisms for soft-sediment deformation: a case study of Late Pleistocene lacustrine sands and clays, Onikobe and Nakayamadaira basins, northeastern Japan. Sedimentology 47: 1211–1226
Kangi A, Aryaei AA, Maasoomi A (2010) Synsedimentary deformations in member 2 of the Mila Formation in the Central Alborz Mountains, Northern Iran. Arab J Geosci 3:33–39
Karlin RE, Abella SEB (1992) Paleoearthquakes in the Pugeot Sound Region recorded in sediments from lake Washington, USA. Science 258:1617–1619
Kastens KA, Cita MB (1981) Tsunami-induced sediment transport in the abyssal Mediterranean Sea. GSA Bull 92(11):845–857
Kastens KA (1984) Earthquakes as a triggering mechanism for debris flows and turbidites on the Calabrian Ridge. Mar Geol 55(1–2):13–33
King LM (1994) Turbidite to storm transition in a migrating foreland basin: the Kendal Group (Upper Silurian), northwest England. Geol Mag 131:255–267
Kneller BC, Branney MJ (1995) Sustained high-density turbidity currents and the deposition of thick massive sands. Sedimentology 42:607–616
Koç-Taşgın C (2011) Seismically-generated hydroplastic deformation structures in the Late Miocene lacustrine deposits of the Malatya Basin, eastern Turkey. Sediment Geol 235:264–276
Koç-Taşgın C, Diniz-Akarca C (2018) Soft-sediment deformation structures related to tectonomagmatic activity: a case study from the borate-bearing lacustrine deposits of early Miocene Bigadiç Basin, NW Turkey. Sediment Geol 373:32–47
Koç-Taşgın C, Türkmen I (2009) Analysis of soft-sediment deformation structures in Neogene fluvio-lacustrine deposits of Çaybağı Formation, eastern Turkey. Sediment Geol 218:16–30
Koç-Taşgın C, Orhan H, Türkmen I, Aksoy E (2011) Soft-sediment deformation structures in the late Miocene Şelmo Formation around Adıyaman area, southeastern Turkey. Sediment Geol 235:277–291
Koç-Taşgın C (2017) Soft-sediment deformation related to syntectonic intraformational unconformity in the early Palaeocene alluvial-fan deposits of Kuşçular Formation in the Elazığ sector of Tauride foreland, eastern Turkey. J Afr Earth Sci 134:665–677
Koç-Taşgın C (2018) Kırkgeçit Formasyonu'nda (Elazığ Çevresi) Gözlenen Yumuşak Çökel Deformasyon Yapılarının Özellikleri ve Oluşumu. TÜBİTAK 116Y017 Nolu Proje raporu 104s

Koç-Taşgın C, Altun F (2019) Denizel Ortamlarda Oluşan Yumuşak Çökel Deformasyon Yapılarına Bir Örnek; Kayma-Oturma Yapıları, Kırkgeçit Formasyonu, KB Baskil, Elazığ. FÜ Müh Bil Derg. 31, 145-156

Koç-Taşgın C, Türkmen İ, Diniz-Akarca C. (2018) Synsedimentary deformation structures on early Miocene lacustrine deposits of the Bigadiç basin (Balıkesir), basal limestone unit. B. Gen. Direct. Min. Research and Exploration (MTA) 156, 67-86

Kuenen PH (1953) Significant features of graded bedding. Bull Am Assoc Pet Geol 37:1044–1066

Kuenen PH (1967) Emplacement of flysch-type sand beds. Sedimentology 9:203–243

Lewis KB (1971) Slumping on a continental slope inclined at 1-4. Sedimentology 16:97–110

Lowe DR (1975) Water escape structures in coarse-grained sediments. Sedimentology 22:157–204

Lowe DR (1976) Grain flow and grain flow deposits. J Sediment Petrol 46:188–199

Lowe DR (1982) Sediment gravity flows, II. Depositional models with special reference to the deposits of high-density turbidity currents. J Sediment Petrol 52:279–297

Marco S, Agnon A (1995) Prehistoric earthquake deformations near Massada, Dead Sea Graben. Geology 23:695–698

Marjanac T (1985) Composition and origin of the megabed containing huge clasts, flysch formation, middle Dalmatia, Yugoslavia. In: Abstracts and Poster Abstracts, 6th European Meeting Int. Assoc. Sedimentologists (Lleida, Spain) pp. 270-273

Mastrogiacomo G, Moretti M, Owen G, Spalluto L (2012) Tectonic triggering of slump sheets in the Upper Cretaceous carbonate succession of the Porto Selvaggio area (Salento Peninsula, southern Italy): synsedimentary tectonics in the Apulion Carbonate Platform. Sediment Geol 269-270:15–27

Mazumder R, van Loon AJ, Malviya VP, Arima M, Ogawa Y (2016) Soft-sediment deformation structures in the Mio-Pliocene Misaki formation within alternating deep-sea clays and volcanic ashes (Miura Peninsula, Japan). Sediment Geol 344:323–335

McClelland HLO, Woodcock NH, Gladstone C (2011) Eye and sheath folds in turbidite convolute lamination: aberystwyth Grits Group, Wales. J Struct Geol 33:1140–1147

Meshram DC, Sangode SJ, Gujar AR, Ambre NV, Dhongle D, Porate S (2011) Occurrence of soft sediment deformation at Dive Agar beach, west coast of India: possible record of the Indian Ocean tsunami (2004). Nat Hazards 57:385–393

Middleton GV (1969) Turbidity currents. In: The New Concepts of Continental Margin Sedimentation. Am Geol Inst Short Course Lecture Notes 10:20

Mills PC (1983) Genesis and diagnostic value of soft-sediment deformation structures — a review. Sediment Geol 35:83–104

Molina JM, Alfaro P, Moretti M, Soria JM (1998) Soft-sediment deformation structures induced by cyclic stress of storm waves in tempestites (Miocene, Guadalquivir Basin, Spain). Terra Nova 10: 145–150

Montenat C, Barrier P, d'Estevou PO, Hibsch C (2007) Seismites: an attempt at critical analysis and classification. Sediment Geol 196: 5–30

Moore DG (1961) Submarine slumps. J Sediment Petrol 31:343–357

Moretti M, Alfaro P, Caselles O, Canas JA (1999) Modeling seismites with a digital shaking table. Tectonophysics 304:369–383

Moretti M, Soria JM, Alfaro P, Walsh A (2001) Asymmetrical soft-sediment deformation structures triggered by rapid sedimentation in turbiditic deposists (late Miocene, Guadix Basin, southern Spain). Facies 46(47):283–294

Morgenstern NR (1967) Submarine slumping and the initiation of turbidity currens In: A. F. Richards(Ed.), Marine Geotechnique Urbana, Ill., University of Illinois Press 189-219

Mulder T, Alexander J (2001) The physical character of subaqueous sedimentary density flow and their deposits. Sedimentology 48(2): 269–299

Mutti E, Ricci Lucchi F (1975) Turbidite facies and facies associations. In: E Mutti et al. (Eds), Examples of Turbidite Facies and Associations from Selected Formations of the Northern Apennines. Field Trip Guidebook A-11, 9th Inter. Association of Sediment. Congr., Nice, pp. 21-36

Naylor MA (1981) Debris flow (olistostromes) and slumping on a distal passive continental margin: the Palombini limestone–shale sequence of the northern Apennines. Sedimentology 28(6):837–852

Neuwerth R, Suter F, Guzman CA, Gorin GE (2006) Soft-sediment deformation in a tectonically active area: the Plio-Pleistocene Zarzal Formation in the Cauca Valley (Western Colombia). Sediment Geol 186:67–88

Obermeier SF (1996) Use of liquefaction-induced features for paleoseismic analysis — an overview of how seismic liquefaction features can be distinguished from other features and how their regional distribution and properties of source sediment can be used to infer the location and strength of Holocene paleo-earthquakes. Eng Geol 44(1–4):1–76

Obermeier SF, Pond EC (1999) Issues in Using Liquefaction Features for Paleoseismic Analysis. Seismol Res Lett 70(1):34–58

Oliveira CM, Hodgson DM, Flint SS (2009) Aseismic controls on in situ soft-sediment deformation processes and products in submarine slope deposits of the Karo Basin, South Africa. Sedimentology 56: 1201–1225

Ortner H, Kilian S (2016) Sediment creep on slopes in pelagic limestones: upper Jurassic of Northern Calcareous Alps, Austria. Sediment Geol 344:350–363

Owen G (1987) Deformationprocesses in unconsolidated sands. In: Jones, M.E., Preston, R.M.F. (Eds.), Deformation of Sediments and Sedimentary Rocks. Geol Soc (London) Spec Pub No. 29: pp. 11–24

Owen G (1995) Soft-sediments deformation in upper proterozoic Torridonian sandstones (applecross formation) at Torridon, northwest Scotland. J Sediment Res A65:495–504

Owen G (2003) Load structures: gravity-driven sediment mobilization in the shallow subsurface. In: Van Rensebergen, P., Hillis, R.R., Maltman, A.J., Morley, C.K. (Eds.), Subsurface Sediment Mobilization, Geol Soc (London) Spec Pub No. 216: pp. 21–34

Owen G, Moretti M (2008) Determining the origin of soft-sediment deformation structures: a case study from Upper Carboniferous delta deposits in south-west Wales, UK. Terra Nova 20:237–245

Özkul M (1988) Elazığ batısında Kırkgeçit Formasyonu üzerinde sedimantolojik incelemeler. Doktora tezi (Yayımlanmamış), F.Ü. Fen Bil. Enst. Elazığ

Özkul M, Kerey E (1996) Şelf, derin-deniz kompleksinde fasiyes analizleri: Kırkgeçit Formasyonu (Orta Eosen-Oligosen) Baskil, Elazığ. Turk J Earth Sci 5:57–70

Papadopoulos GA, Yalçiner AC, Kuran U (1994) A discussion on the generation mechanism of 1956 Southern Aegean Tsunami. Assembly of European Geophysical Society, Tsunami Session, 23-27 April, 1994, Grenoble, France

Perinçek D (1979) Palu-Karabegan-Elazıg-Sivrice-Malatya alanının jeolojisi ve petrol imkanları. TPAO Arsivi Raporu no:1361 (Yayınlanmamıs) Ankara

Perissoratis C, Mitropoulos D, Angelopoulos I (1984) The role of earthquakes in inducing sediment mass movements in the eastern Korinthiakos Gulf. An example from the February 24–March 4, 1981 activity. Mar Geol 55:35–45

Pickering KT (1982) Middle-fan deposits from the late Precambrian Kongsfjord Formation Submarine Fan, northeast Finnmark, northern Norway. Sediment Geol 33:79–110

Pickering KT (1986) Wet-sediment deformation in the Upper Ordovician Point Leamington Formation: possible foreland basin

sedimentation. Notre Dame Bay, north-central Newfoundland. In: M.E. Jones (Editor), Deformation mechanisms in sedimentary rocks. Geol Soc Lond Spec Pub 199-225

Pickering KT, Stow DAV, Watson MP, Hiscott RN (1986) Deep-water facies, processes and models: a review and classification scheme for modern and ancient sediments. Earth-Sci Rev 23:75–174

Rodríguez-Pascua MA, Calvo JP, De Vicente G, Gómez-Gras D (2000) Soft-sediment deformation structures interpreted as seismites in lacustrine sediments of the Prebetic Zone, SE Spain, and their potential use as indicators of earthquake magnitudes during the late Miocene. Sediment Geol 135:117–135

Rossetti DF (1999) Soft-sediment deformation structures in late Albian to Cenomanian deposits, Sao Luis Basin, northern Brazil: evidence for palaeoseimicity. Sedimentology 46:1065–1081

Rossetti DF, Goes AM (2000) Deciphering the sedimentological imprint of paleoseismic events: an example from the aptian codo formation, northern Brazil. Sediment Geol 135:137–156

Rossetti DF, Santos AE (2003) Events of sediment deformation and mass failure in Upper Cretaceous estuarine deposits (Cameta´ Basin, northern Brazil) as evidence for seismic activity. Sediment Geol 161:107–130

Rossetti DF, Goes AM, Truckenbrodt W, Anaisse J (2000) Tsunami-induced large-scale scour-and-fill structures in late albian to cenomanian deposits of the grajau basin, northern Brazil. Sedimentology 47:309–323

Rossetti DF, Alves FC, Valeriana MM (2017) A tectonically-triggered late Holocene seismite in the southern Amazonian lowlands, Brazil. Sediment Geol 358:70–83

Şengör AMC (1980) Principles of the neotectonics of Turkey. Turkish Geological Society Publication, p. 40 (in Turkish)

Şengör AMC, Yılmaz Y (1983) Evolution of Neo-Tethyan in Turkey. Turkish Geological Society Special Publication p. 75 (in Turkish)

Saxov S, Nieuwenhuis JK (1982) Marine slides and other mass movements NATO Conf. Ser. IV: Marine Sci. Plenum Press, New York, 353 pp

Schnellmann M, Anselmetti Flavio S, Giardini D, McKenzie JA, Ward SN (2002) Prehistoric earthquake history revealed by lacustrine slump deposits. Geology 30:1131–1134

Scott B, Price S (1988) Earthquake-induced structures in young sediments. Tectonophysics 147:165–170

Seilacher A (1969) Fault-graded beds interpreted as seismites. Sedimentology 13:155–159

Seilacher A (1984) Sedimentary structures tentatively attributed to seismic events. Mar Geol 55:1–12

Shanmugam G (2016) Slides, slumps, debris flows, turbidity currents, and bottom currents. Reference Module in Earth Systems and Environmental Sciences Publisher: Elsevier

Shiki T, Cita MB (2008) Tsunami-related sedimentary properties of Mediterranean homogenites as an example of deep-sea tsunamite. In: Shiki T, Tsuji Y, Yamazaki T, Minoura K (eds) Tsunamiites-Features and Implications, 203–215. Elsevier, Amsterdam

Sims JD (1975) Determining earthquake recurrence intervals from deformational structures in young lacustrine sediments. Tectonophysics 29(1–4):141–152

Smith DE, Foster IDL, Long D, Shi S (2007) Reconstructing the pattern and depth of onshore in a paleotsunami from associated deposits. Sediment Geol 200(3–4):362–371

Spalluto L, Moretti M, Festa V, Tropeano M (2007) Seismically-induced slumps in Lower-Maastrichtian peritidal carbonates of the Apulian platform (southern Italy). Sediment Geol 196:81–98

Stanley DJ, Palmer HD, Dill RF (1978) Coarse sediment transport by mass flow and turbidity currents processes and downslope transformation in Annot sandstone canyon-fan valley systems. In: DJ Stanley and G Keeling (Eds.), Sedimentation in Submarine Canyons, Fans, and Trenches, Dowden, Hutchinson and Ross Stroudsburg Penn, pp 85-115

Stow DAV, Cremer M, Droz L et al. (1986) Facies, composition and texture of Mississippi fan sediments, DSDP Leg 96, Gulf of Mexico. In: A.H. Bouma, J. Coleman et al., Init. Repts. DSDP 96. U.S. Print. Office, Washington, D.C

Stromberg SG, Bluck B (1998) Turbidite facies, fluid-escape structures and mechanisms of emplacement of the Oligo-Miocene Aljibe Flysch, Gibraltar Arc, Betics, southern Sapin. Sediment Geol 115: 267–288

Tinterri R, Muzzi Magalhaes P, Tagliaferri A, Cunha RS (2016) Convolute laminations and load structures in turbidites as indicators of flow reflections and decelerations against bounding slopes. Examples from the Marnoso-arenacea Formation (northern Italy) and Annot sandstones (south eastern France). Sediment Geol 344: 382–407

Turan M (1984) Baskil Aydınlar (Elazığ) Yöresinin stratigrafisi ve tektoniği. Doktora Tezi (Yayımlanmamış), F.Ü Fen Bil. Enst., Elazığ

Turan M (1993) Elazığ yakın civarındaki bazı önemli tektonik yapılar ve bunların bölgenin jeolojik evrimindeki yeri. In: Kazancı N (ed.) Suat Erk Jeoloji Sempozyumu Bildirileri. Ankara, pp 193–204

Turan M, Aksoy E, Bingöl AF (1995) Doğu Torosların Jeodinamik Evriminin Elazığ Civarındaki Özellikleri. Fırat Üniv Fen Müh Bil Der 7(2):177–199

Türkmen İ, Ertürk Y (2002) Kırkgeçit Formasyonu'nun (Orta Eosen-Oligosen) Akuşağı Köyü (Baskil-Elazığ) dolaylarındaki yüzeylemelerinin sedimantolojik özellikleri. Türkiye Petrol Jeol Der Bül 14(2):1–16

Türkmen İ, Esen N (1997) Şelf, kanyon ve havza düzlüğü kompleksinin fasiyes özellikleri: Kırkgeçit Formasyonu (Orta Eosen-Oligosen), Elazığ çevresi, Türkiye. Fırat Üniv Fen Müh Bil Der 9(2):107–123

Türkmen İ, İnceöz M, Aksoy E, Kaya M (2001) Elazığ yöresinin Eosen stratigrafisi ve paleocografyası ile ilgili yeni bulgular. H.Ü. Yerbilimleri 24:81–95

Valente A, Slaczka A, Cavuoto G (2014) Soft-sediment deformation structures in seismically affected deep-sea Miocene turbidites. Geologos 20:67–78

Vanneste K, Meghraoui M, Camelbeek T (1999) Late Quaternary earthquake-related soft-sediment deformation along the Belgian portion of the Feldbiss Fault, Lower Rhine Graben system. Tectonophysics 309:57–79

Visher GS, Cunningham RD (1981) Convolute laminations – a theoretical analysis: example of Pennsylvanian sandstone. Sediment Geol 28:175–189

Watkins JS, Montadert L, Dickerson PW (Editors) (1979) Geological and geophysical investigations of continental margins. Am Assoc Petrol Geol Mem 29: 472 pp

Watson MP (1981) Submarine fan deposits of the Upper Ordovician-Lower Silurian milliners arm formation, New World Island, Newfoundland. Unpub. Ph.D. Thesis, Oxford Univ, Oxford

Yamamoto Y (2014) Dewatering structure and soft-sediment deformation controlled by slope instability: examples from the late Miocene to Pliocene Miura–Boso accretionary prism and trench-slope basin, central Japan. Mar Geol 356:65–70

Yang R, Van Loon AJ (2016) Early Cretaceous slumps and turbidites with peculiar soft-sediment deformation structures on Lingshan Island (Qingdao, China) indicating a tensional tectonic regime. J Asian Earth Sci 129:206–219

Yazgan E (1984) Geodyamic evolution of the Eastern Taurus region. In: Tekeli O, Göncüoğlu MC (eds) . Geolgy of the Taurus Belt, Ankara, pp 199–208

Yazgan E, Chessex R (1991) Geology and tectonic evolution of the Southeastern Taurides in the region of Malatya. The Bull Turkish Assoc Petrol Geol 3(1):1–42